ISBN: 978-9940-46-042-6

SCIENCE AND MATHEMATICS SCIENCES

IVPE 2020

SCIENCE AND MATHEMATICS SCIENCES

Theory, Current Researches and New Trends

Assoc. Prof. Dr. Mehtap Düz

IVPE 2020

SCIENCE AND MATHEMATICS SCIENCES

Theory, Current Researches and New Trend

Editor
Assoc. Prof. Dr. Mehtap DÜZ

Editor
Assoc. Prof. Dr. Mehtap DÜZ

First Edition •© October 2020 /Cetinje-Montenegro

ISBN • 978-9940-46-042-6

web: www.ivpe.me

Tel. +382 41 234 709

e-mail: office@ivpe.me

Cetinje, Montenegro

PREFACE

The "SCIENCE AND MATHEMATICS SCIENCE" book covers interdisciplinary research focusing on current studies for academics and researchers working in the field of science and mathematics. The book is a resource to inform readers about current topics in natural sciences and mathematics. In this book, academicians working in different fields share their studies with the scientific community. Thus, more researchers will be aware of these studies and have some new ideas for their future work. Selected sections have been approved for publication by expert referees.

The authors who submitted their work to the preparation of this book made valuable contributions without expecting anything in return. Thank you for their contribution. I would like to thank IVPE Publishing House, who used all their material and moral means in bringing the book to the world of science, its valuable managers and the team that performed the arrangement of the book with great patience and skill.

Assoc. Prof. Dr. Mehtap DÜZ

CONTENTS

REFEREES

Prof. Dr. Halit Demir, Van Yüzüncü yıl University, Turkey

Prof. Dr. Rıdvan Karapınar, Burdur Mehmet Akif Ersoy University, Turkey

Prof. Dr. Tanja Soldatovic, Novi Pazar State University, Serbia

Assoc. Prof. Dr. Mehtap Düz, İnönü University, Turkey

CHAPTER I

SYNTHESIS AND CHARACTERIZATION OF BENZOTHIAZOLIUM SALTS CONTAINING SUBSTITUTED BENZYL GROUPS

Dr. Deniz DEMİR ATLI

Manisa Celal Bayar University, Manisa, Turkey, e-mail: deniz.demir@cbu.edu.tr
Orcid No: 0000-0001-8442-4916

1. Introduction

N-heterocyclic carbenes (NHCs) have strong σ-donating and weak π-accepting characters. They are alternative to phosphine ligands because of these properties. The first crystalline NHC was synthesized in 1991 (Arduengo et al., 1991). Since then, numerous studies have been performed on NHC complexes (Baron et al., 2020; Soliev et al., 2020; Demir Atli, 2020; Li et al., 2020; Berti et al., 2020; Io et al., 2020; Nguyen et al., 2020; Abubakar et al., 2020; Reddy et al., 2020). This intense interest in NHC complexes stems from the catalytic application of these compounds with strong metal-carbon bonds. However, the studies on the development of the carbenes comprising different kinds of heterocycles have been needed in recent times. This requirement brought about the new types of N,X-heterocyclic carbenes (X = P, O, S, etc.).

In former study about N,S-heterocyclic carbenes (NSHCs), vitamin B_1 was employed to catalyze the benzoin condensation reactions (Breslow, 1958). Existence of sulphur which is more electropositive and softer than nitrogen proffers an alternating in catalyst designing to the use of bulky substituents on nitrogen in NSHC ligands. Some of the reports regarding using of transition metal complexes containing benzothiazol-2-ylidene ligands as catalysts are as follows: Ru(II) complexes in transfer hydrogenation of carbonyls and transfer hydrosilylation (Oruc et al., 2016; Ding et al., 2010; Ding et al., 2011; Ding et al., 2012a), Pd(II) complexes in Heck coupling and Suzuki coupling (Yen et al., 2006; Yen et al., 2008; Yen et al., 2009), Ni(II) complexes in Ullmann coupling (Ding et al., 2012b) and Cu(I) complexes in Huisgen 1,3-dipolar cycloaddition of azides and alkynes (Han et al., 2014). NSHC Au(I) complexes were reported to show cytotoxic activity (Gutierrez et al., 2014).

In this study, preparation of a series of benzothiazolium salts are reported. Structures of the synthesized compounds are solved by FT-IR, NMR and elemental analysis techniques.

2. Experimentral

2.1. General comments

All experiments were performed in air. Benzothiazole was used after distillation. Except this, the other chemicals and the solvents were used without any purification. Elemental analysis and NMR analyses were actualized by a CHNS-932 (LECO) elemental analyzer and a Varian 400 MHz NMR spectrophotometer, respectively. FT-IR spectrum was observed by Perkin Elmer spectrophotometer. Melting points were recorded with Electrothermal 9100 device.

2.2. Synthesis of benzothiazolium salts

2.2.1. N-(3,5-dimethoxybenzyl)benzothiazolium bromide (1)

The mixture of benzothiazole (0.33 g, 2.43 mmol) and 3,5-dimethoxybenzyl bromide (0.56 g, 2.43 mmol) was stirred in DMF (3 mL) at 80 °C for 24h. After cooling to the room temperature, Et_2O was added. After filtration, the solids were excess Et_2O. Yield: 0.68 g, 77%. m.p.: 210-211 °C. ν_{CN}: 1596 cm^{-1}. ^1H NMR (400 MHz, dmso-d_6): δ = 3.71 (s, 6H, OMe), 6.03 (s, 2H, NCH_2), 6.50 (s, 1H, Ar-H), 6.70 (s, 2H, Ar-H), 7.85 (dt, J_1 = 26.0 Hz, J_2 = 7.3 Hz, 2H, Ar-H), 8.33 (d, J = 8.3 Hz, 1H, Ar-H), 8.53 (d, J = 8.2 Hz, 1H, Ar-H), 10.77 (s, 1H, NCHS) ppm. ^{13}C NMR (100 MHz, dmso-d_6): δ = 55.63, 55.83 (NCH_2, OMe), 100.66, 107.55, 118.81, 125.90, 129.33, 130.58, 132.22, 136.50, 142.13, 162.16 (Ar-C), 166.10 (NCS) ppm. Anal. Calcd. for $C_{16}H_{16}NO_2SBr$(%): C, 52.46; H, 4.41; N, 3.82; S, 8.75. Found: C, 52.16; H, 4.54; N, 3.93; S, 8.16.

2.2.2. N-(3,5-di-tert-butylbenzyl)benzothiazolium bromide (2)

Compound **2** was prepared in the same way as compound **1** using benzothiazole (0.18 g, 1.36 mmol) and 3,5-di-tert-butylbenzyl bromide (0.38 g, 1.36 mmol). Yield: 0.40 g, 70%. m.p.: 217-218 °C. ν_{CN}: 1600 cm^{-1}. ^1H NMR (400 MHz, dmso-d_6): δ = 1.20 (s, 18H, Bu^t), 6.06 (s, 2H, NCH_2), 7.35 (s, 1H, Ar-H), 7.42 (s, 2H, Ar-H), 7.77-7.83 (m, 1H, Ar-H), 7.85-7.91 (m, 1H, Ar-H), 8.46 (d, J =8.2 Hz, 1H, Ar-H), 8.52 (d, J =8.3 Hz, 1H, Ar-H),10.75 (s, 1H, NCHS) ppm. ^{13}C NMR (100 MHz, dmso-d_6): δ = 30.94, 36.06 (Bu^t), 56.15 (NCH_2), 118.40, 122.99, 123.59, 125.90, 128.94, 132.23, 132.31, 140.60, 142.86, 151.69 (Ar-C), 165.15 (NCS) ppm. Anal. Calcd. for $C_{22}H_{28}NSBr$(%): C, 63.14; H, 6.76; N, 3.35; S, 7.66. Found: C, 62.60; H, 6.78; N, 3.29; S, 7.32.

2.2.3. N-(3,5-dimethylbenzyl)benzothiazolium bromide (3)

Compound **3** was prepared in the same way as compound **1** using benzothiazole (0.43 g, 3.20 mmol) and 3,5-dimethylbenzyl bromide (0.64 g, 3.20 mmol). Yield: 0.98 g, 91%. m.p.: 244-245 °C. ν_{CN}: 1600 cm^{-1}. ^1H NMR (400 MHz, dmso-d_6): δ = 2.19 (s, 6H, Me), 6.03 (s, 2H, NCH_2), 6.97 (s, 1H, Ar-H), 7.09 (s, 2H, Ar-H), 7.76-7.88 (m, 2H, Ar-H), 8.27 (d, *J* = 8.0 Hz, 1H, Ar-H), 8.53 (d, *J* = 8.0 Hz, 1H, Ar-H), 10.80 (s, 1H, NCHS) ppm. ^{13}C NMR (100 MHz, dmso-d_6): δ = 21.23 (Me), 57.11 (NCH_2), 116.68, 125.89, 126.36, 126.52, 128.30, 128.85, 129.90, 130.07, 130.86, 131.06, 132.25, 133.06, 137.58, 138.29, 138.75, 140.48, 146.16, 163.91 (Ar-C), 166.10 (NCS) ppm. Anal. Calcd. for $C_{16}H_{16}NSBr$(%): C, 57.48; H, 4.83; N, 4.19; S, 9.59. Found: C, 57.49; H, 4.78; N, 4.15; S, 9.44.

2.2.4. N-(3-methoxybenzyl)benzothiazolium chloride (4)

Compound **4** was prepared in the same way as compound **1** using benzothiazole (0.33 g, 2.42 mmol) and 3-methoxybenzyl chloride (0.36 mL, 2.42 mmol) except that it was performed in solvent-free medium. Yield: 0.35 g, 49%. m.p.: 155-156 °C. ν_{CN}: 1600 cm^{-1}. ^1H NMR (400 MHz, dmso-d_6): δ = 3.72 (s, 3H, OMe), 6.12 (s, 2H, NCH_2), 6.93 (dd, J_1 = 2.6 Hz, J_2 = 8.3 Hz, 1H, Ar-H), 7.02 (d, *J* = 7.9 Hz, 1H, Ar-H), 7.18 (s, 1H, Ar-H), 7.30 (t, *J* = 7.4 Hz, 1H, Ar-H), 7.77-7.89 (m, 2H, Ar-H), 8.32 (d, *J* = 8.2 Hz, 1H, Ar-H), 8.53 (d, *J* = 8.0 Hz, 1H, Ar-H), 10.95 (s, 1H, NCHS) ppm. ^{13}C NMR (100 MHz, dmso-d_6): δ = 55.48, 55.67 (NCH_2, OMe), 114.71, 114.85, 117.87, 120.765, 125.932, 128.90, 130.06, 130.74, 132.31, 135.13, 141.34, 160.89 (Ar-C), 166.89 (NCS) ppm. Anal. Calcd. for $C_{15}H_{14}NOSCl{\cdot}H_2O$(%): C, 58.14; H, 5.22; N, 4.52; S, 10.35. Found: C, 57.89; H, 5.18; N, 4.40; S, 10.25.

3. Results and discussion

Synthesis methods for the compounds **1-4** are given in Scheme 1 and Scheme 2. Benzothiazolium bromide salts **1-3** were synthesized in high yields by the reaction of benzothiazole with one equivalent of substituted benzyl bromides in DMF at 80 °C. Since this method led to the chloride salt **4** in very low yield, this compound was prepared in solvent-free condition in 49% yield. All the synthesized compounds are stable towards air and moisture. These are soluble in water, methanol, ethanol, DMSO, DMF and insoluble Et_2O, n-hexane, THF.

Being the experimental elemental analysis results consistent with the theoretical values shows that the expected compounds were achieved. Stretching frequencies related to C=N bond were observed at 1596-1600 cm^{-1}. NMR data suggest the structures of the benzothiazolium salts **1-4**

(Fig. 1-4). Acidic C2 protons and carbons are observed at 10.75-10.95 ppm and 165-167 ppm in the ^{1}H NMR and ^{13}C NMR spectra, respectively. The signals related to the methylene groups bound to nitrogen atom resonate around at 6.0 ppm.

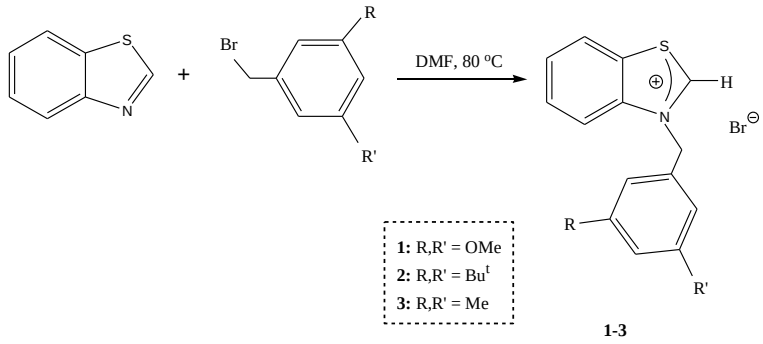

Scheme 1. Synthesis of **1-3**

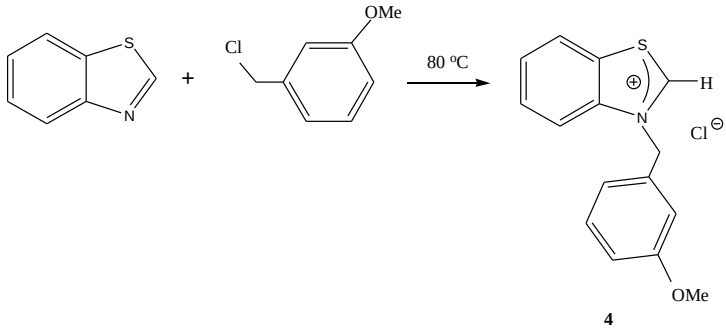

Scheme 2. Synthesis of **4**

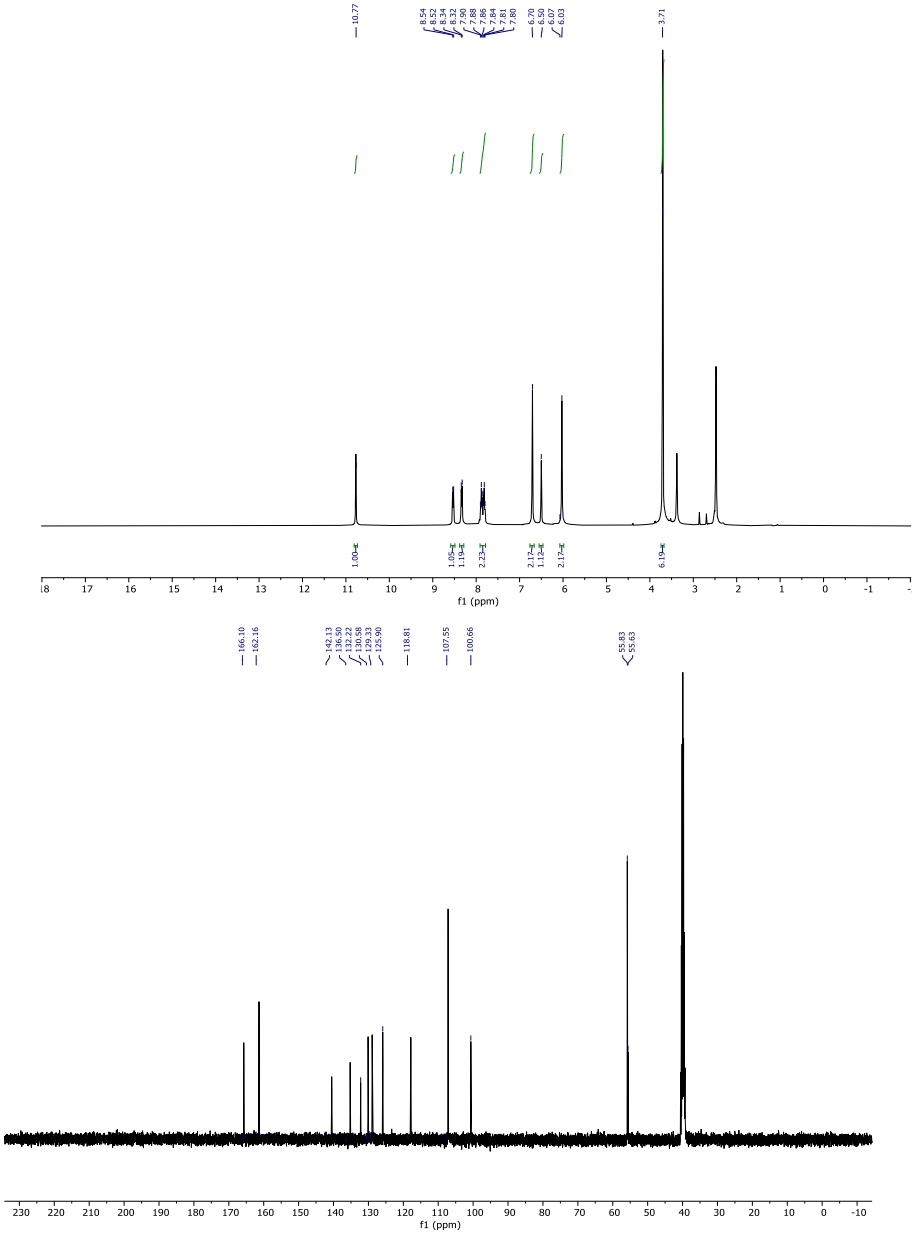

Fig. 1 ^{1}H NMR and ^{13}C NMR spectra of **1**

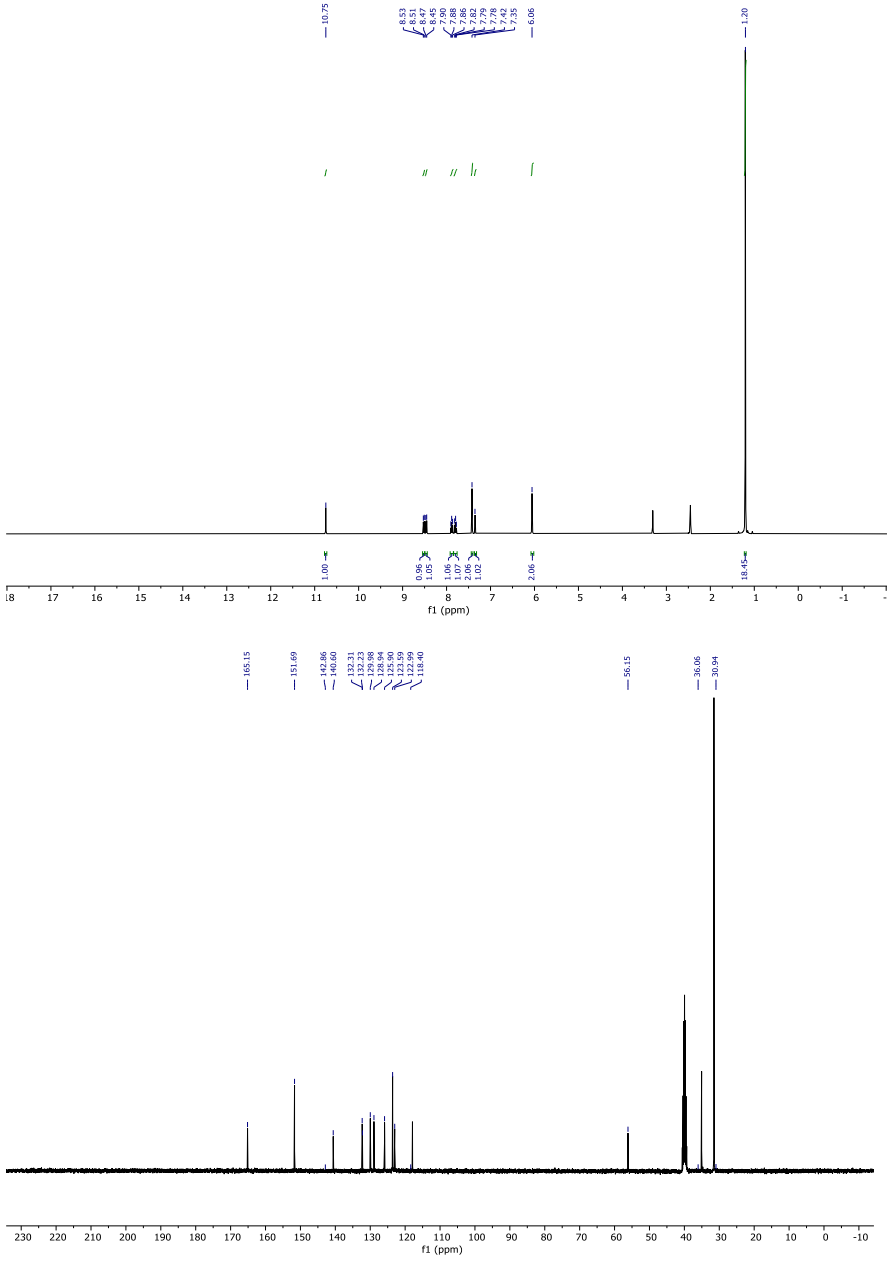

Fig. 2 ^{1}H NMR and ^{13}C NMR spectra of **2**

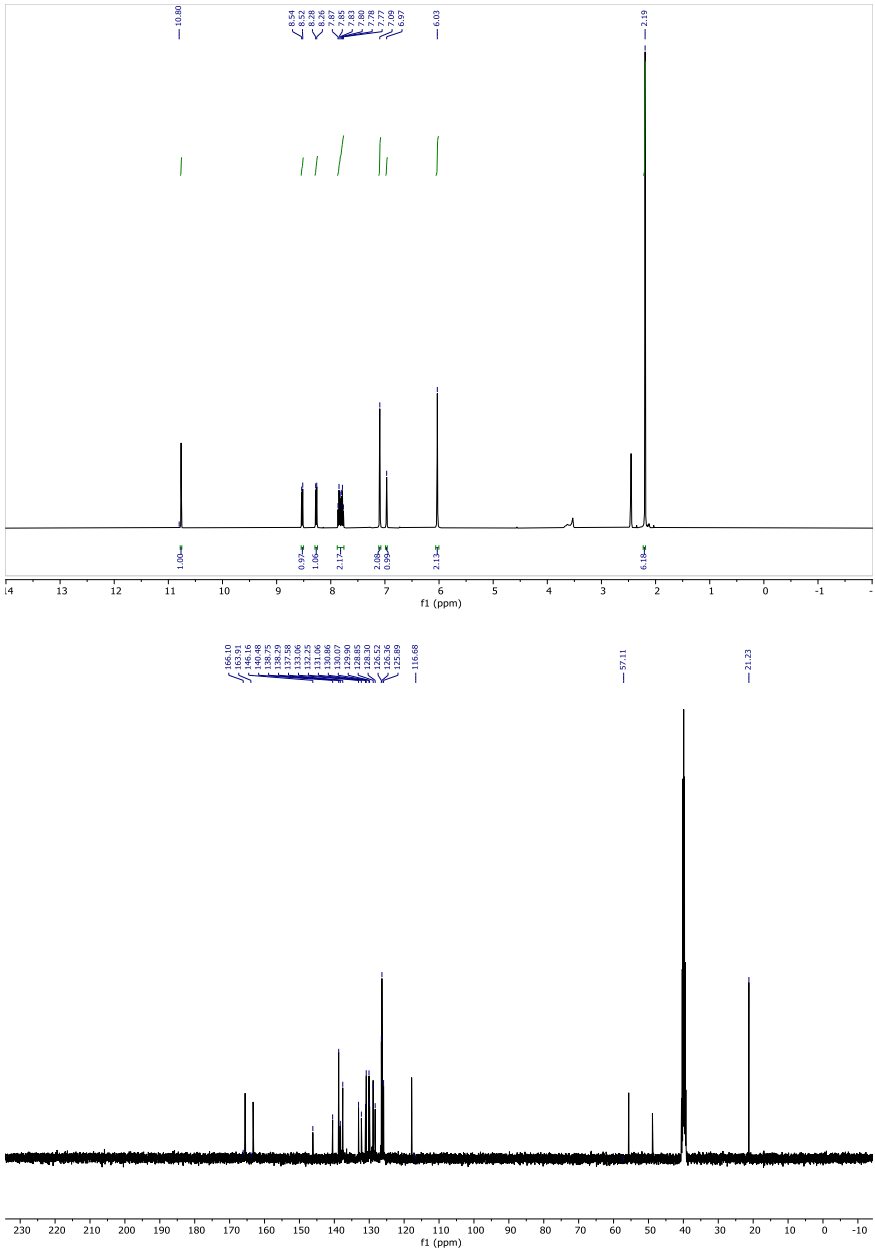

Fig. 3 ^{1}H NMR and ^{13}C NMR spectra of **3**

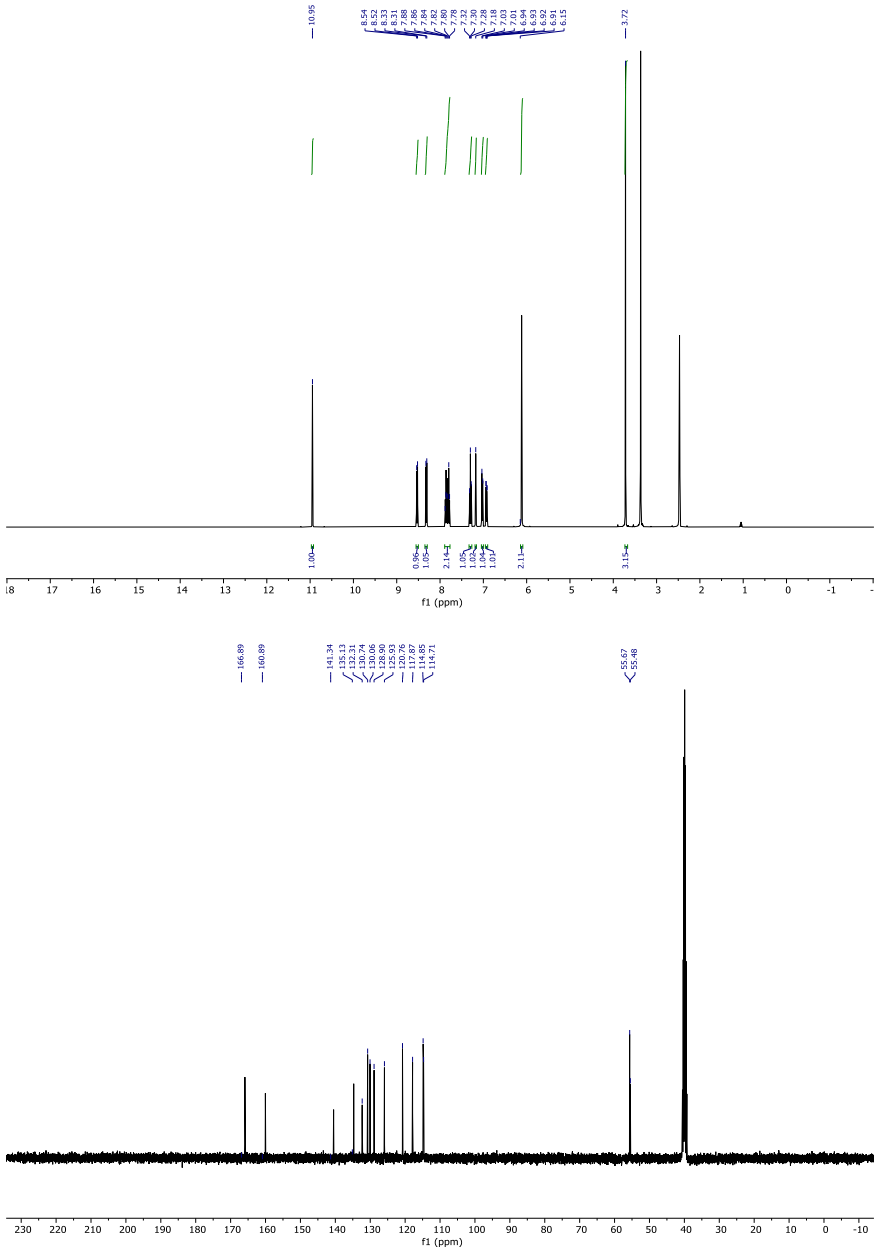

Fig. 4 ^{1}H NMR and ^{13}C NMR spectra of **4**

4. Conclusions

In this study, N-(3,5-dimethoxybenzyl)benzothiazolium bromide, N-(3,5-di-tert-butylbenzyl)benzothiazolium bromide, N-(3,5-dimethyl-benzyl)benzothiazolium bromide and N-(3-methoxybenzyl)benzo-thiazolium chloride salts were accomplishedly prepared and their structures were determined. The studies on the preparation metal complexes to be used as catalysts in some reactions have gone on.

Acknowledgements

This work was supported by the Scientific Research Project Fund of Manisa Celal Bayar University under the project number 2019-141.

References

Abubakar, S., Bala, M.D., Transfer hydrogenation of ketones catalyzed by symmetric imino-N-heterocyclic carbene Co(III) complexes, ACS Omega, Vol.5, No.6 (2020), pp.2670-2679.

Arduengo, A.J., Harlow, R.L., Kline, M., A stable crystalline carbene, Journal of American Chemical Society, Vol.113, No.1 (1991), pp.361-363.

Baron, M., Dall′Anese, A., Miolato, A., Cairoli, M.L.C., Di Marco, V., Graiff, C., Pothig, A., Tubaro, C., New homoleptic gold carbene complexes via Ag-Au transmetalation: synthesis and application of [Au(diNHC)(2)](3+) cations as H-1-NMR and UV-vis halide sensors, New Journal of Chemistry, Vol.44, No.14 (2020), pp.5343-5353.

Berti, B., Bortoluzzi, M., Cesari, C., Femoni, C., Lapalucci, M.C., Mazzoni, R., Zacchini, S., A comparative experimental and computational study of heterometallic Fe-M (M = Cu, Ag, Au) carbonyl clusters containing N-heterocyclic carbene ligands, European Journal of Inorganic Chemistry, Vol.2020, No.22 (2020), pp.2191-2202.

Breslow, R., On the mechanism of thiamine action. IV.1 Evidence from studies on model systems, Journal of American Chemical Society, Vol.80, No.14 (1958), pp.3719-3726.

Demir Atli, D., Synthesis and catalytic application of cyclopentadienyl nickel(II) N-heterocyclic carbene complexes, Journal of Coordination Chemistry, Vol.73, No.10 (2020), pp.1530-1537.

Ding, N., Hor, T.S.A., Ruthenium(II) N,S-heterocyclic carbene complexes and transfer hydrogenation of ketones, Dalton Transactions, Vol.39, No.42 (2010), pp.10179-10185.

Ding, N., Hor, T.S.A., Syntheses and of ruthenium(II) N,S-heterocyclic carbene diphosphine complexes and their catalytic activity towards transfer hydrogenation, Chemistry-An Asian Journal, Vol.6, No.6 (2011), pp.1485-1491.

Ding, N., Zhang, W., Hor, T.S.A., One-step entry to olefin-tethered N,S-heterocyclic carbene complexes of ruthenium with mixed ligands, Dalton Transactions, Vol.41, No.19 (2012), pp.5988-5994.

Ding, N., Zhang, W., Hor, T.S.A., Formation and crystallographic elucidation of stable [4 + 2]-coordinate nickel(II) N,S-heterocyclic carbene (NSHC) complexes, Dalton Transactions, No.10 (2012), pp.1853-1858.

Gutierrez, A., Gimeno, MC., Marzo, I., Metzler-Nolte, N., Synthesis, characterization, and cytotoxic activity of AuI N,S-heterocyclic carbenes derived from peptides containing L-thiazolylalanine, European Journal of Inorganic Chemistry, Vol.2014, No.15 (2014), pp.2512-2519.

Han, X., Weng, Z., Young, D.J., Jin, G.-X., Hor, T.S.A., Stoichiometric sensitivity and structural diversity in click-active copper(I) N,S-heterocyclic carbene complexes, Dalton Transactions, Vol.43, No.3 (2014), pp.1305-1312.

Io, K.W., Ng, S.W., Yeung, C.F., Wong, C.Y., Synthesis, spectroscopic and computational studies of rhodium(III) complexes bearing N-heterocyclic carbene-based C boolean and N boolean and C pincer ligand and bipyridine/terpyridine, European Journal of Inorganic Chemistry, Vol.2020, No.24 (2020), pp.2343-2351.

Li, J.Y., Wang, L.D., Zhao, Z.F., Li, X.Y., Yu, X., Huo, P.H., Jin, Q.H., Liu, Z.W., Bian, Z.Q., Huang, C.H., Two-coordinate copper(I)/NHC complexes: Dual emission properties and ultralong room-temperature phosphorescence, Angewandte Chemie International Edition, Vol.59, No.21 (2020), pp.8210-8217.

Nguyen, V., Dang, T.T., Nguyen, H.H., Huynh, H.V., Platinum(II) 1,2,4-triazolin-5-ylidene complexes: Stereoelectro-nic influences on their catalytic activity in hydroelementation reactions, Organometallics, Vol.39, No.12 (2020), pp.2309-2319.

Oruc, Z.I. Gok, L., Turkmen, H., Sahin, O., Buyukgungor, O., Cetinkaya, B., Piano-stool benzothiazol-2-ylidene Ru(II) complexes for effective transfer hydrogenation of carbonyls, Journal of Organometallic Chemistry, Vol.807 (2016), pp.36-44.

Reddy, M.V.K., Anusha, G., Reddy, P.V.G., Sterically enriched bulky 1,3-bis(N,N '-aralkyl)benzimidazolium based Pd-PEPPSI complexes for Buchwald-Hartwig amination reactions, New Journal of Chemistry, Vol.44, No.27 (2020), pp.11694-11703.

Soliev, S.B., Astakhov, A.V., Pasyukov, D.V., Chernysev, V.M., Nickel(ii) N-heterocyclic carbene complexes as efficient catalysts for the Suzuki-Miyaura reaction, Russian Chemical Bulletin, Vol. 69 (2020), pp.683-690.

Yen, S.K., Koh, L.L., Hahn, F.E., Huynh, H.V., Hor, T.S.A., Convenient entry to mono- and dinuclear palladium(II) benzothiazolin-2-ylidene complexes and their activities toward Heck coupling, Organometallics, Vol.25, No.21 (2006), pp.5105-5112.

Yen, S.K., Koh, L.L., Huynh, H.V., Hor, T.S.A., Pd(II) complexes with mixed benzothiazolin-2-ylidene and phosphine ligands and their catalytic activities toward C–C coupling reactions, Dalton Transactions, No.5 (2008), pp.699-706.

Yen, S.K., Koh, L.L., Huynh, H.V., Hor, T.S.A., Structures and Suzuki-coupling of N-heterocyclic carbene complexes of PdII with coordinated solvent and PPh3, Australian Journal of Chemistry, Vol.62, No.9 (2009), pp.1047-1053.

CHAPTER II

HEAVY METAL EXPOSURE OF WORKERS WORKING AT PETROLEUM PRODUCTS FILLING STATIONS AND ITS EFFECTS ON REDUCED GSH ENZYME LEVEL

Assist. Prof. Dr. Tülay GÜRSOY

Van Yüzüncü Yıl University, Faculty of Science, Department of Chemistry. Van, TURKEY. tulaygursoy@yyu.edu.tr
Orcid No:0000-0001-6166-6875

Assoc. Prof. Dr. Nurhayat ATASOY

Van Yüzüncü Yıl University, Faculty of Science, Department of Chemistry. Van, TURKEY. nuratasoy@yyu.edu.tr
Orcid No:0000-0002-2171-3396

1. INTRODUCTION

Increased levels of heavy metals in the environment in which they live cause heavy metal levels in most living tissues (Dietz et al. 2009:6128). The sources of heavy metals are the rocks in the earth's crust. For this reason, the metal concentration in the living environment is determined by the elements exist in the composition of the rock species common to this region (Çiftçi et al. 2008:49). The concentration of heavy metals in the natural earth's crust are increased by industrial activities, exhausts of motor vehicles, mineral deposits and enterprises, volcanic activities, fertilizers and pesticides used in agriculture and urban wastes (Asri and Sönmez 2006:36; Jarup 2003:168; Wong and Lye 2008:31).

Free radicals are high-energy, non-stable compounds containing electrons that do not form one or more pairs in their outer atomic orbitals. This undoubted electron causes a great deal of reactivity to free radicals and led them damage many biological materials such as proteins, lipids, DNA and nucleotide coenzymes. Oxidative stress due to heavy metals is a negative change in ROS (reactive oxygen species) production and biological system ROS/RNS (reactive nucleus species) mediated damage and repair balance. In contrast, preventive systems such as glutathione (GSH), paraoxonase (PON), catalase (CAT) and superoxide dismutase

(SOD) in the antioxidant category have the function of eliminating free radicals (Al-Fartosy et al. 2017:83).

Glutathione (GSH), a major reducing agent and antioxidant, is easily oxidized, as it contains an amino group in its structure, a sulfhydride group (-SH), two peptide bonds and carboxylic acid groups and is, therefore, plays a role in many biochemical and pharmacological events (Parcell 2002:23).

Zinc (Zn) is the second trace element in the human body which is the most abundant after iron. Being an essensial element, zinc is necessary for many metaloenzyme functions such as superoxide dismutase, carbonic anhydrase, alcohol dehydrogenase and it works as a cofactor for more than 200 enzymes (ATSDR 2005).

Sources of lead (Pb) exposure mainly include waste spreaded from industrial processes, petroleum products and waste, food, cigarettes, plumbing pipes and local resources (batteries, toys, etc.) (Jaishankar et al. 2014:60).

Cadmium element is found in automotive oils and diesel fuels. Cadmium acetate chemical compound is used in the refining process to remove crude oil and benzene mercaptans. The element of cadmium is spread to air during the filling and combustion of petroleum products and passes to the hair by contact and to the lungs by inhalation (Luckett et al. 2012:181).

Chromium (Cr) belongs to VIA group, and being a transition metal exhibits multible oxidation states from 0 to VI. Cr element is an essential element and plays an important role in glucose, fat and protein metabolism by increasing the effect of insulin in Cr (III) form (Waseem et al. 2014:23). However, International Agency for Research on Cancer (IARC) and the United States Enviromental Protection Agency (USEPA) have reported that high Cr exposure is carcinogenic, while Dangerous Substance Directive (DSD) classifies chromium as a potentially toxic element in both chronic and acute exposure (Grevatt 1998; Commision 1967). Due to the aforementioned properties, in our study, we have given preference Zn (II), Pb (II), Cd (II), and Cr (II) elements and quantified the amount of these elements.

In the present study, we aimed to measure the levels of Zn (II), Pb (II), Cd (II), and Cr (II) and to measure levels of reduced GSH in hair tissues and blood serum samples of workers employed in petroleum products filling stations in Van province of Turkey for determining the effect of heavy metals on abovementioned antioxidant enzyme.

2. MATERIALS AND METHODS

2.1. Specimens

A total of 42 petrol stations workers (research group- 42 male) were retrospectively included in this research from 12 petrol stations in Van province of Turkey between 2015 and 2018. All members of the research group were working on alternate days (24 hours) for the filling of petroleum products and were identical according to eating habits, body weight and sex between each other and the control group. Only unleaded fuel-95, diesel fuel, and liquid petroleum gas (LPG) were used in all included stations. A different marker was added into the diesel fuel to increase the efficacy in each petroleum station. The control group consisted of 25 age- and sex-matched healthy individuals based on the following criteria: eating habits, age, body weight, sex, and 25 individuals living in the city center (about $\geq$ 5 km far from petrol stations) and working in the office work were included. Those (research and control group) who used alcohol or any other medication (including antioxidant medications) and those with accompanying metabolic disorder were excluded. A written informed consent was obtained from each participant. The study protocol was approved by the local Ethics Committee (Date: 05.05.2015 / No: 02). The study was conducted in accordance with the principles of the Declaration of Helsinki.

2.1.2. Blood collection

Venous blood samples were collected early in the morning following 9-12-hour fasting from all participants. The samples were centrifuged for 10 min at 4,000 rpm/min, and sera were separated. Serum samples were kept at -80°C until biochemical analysis.

2.1.3. Hair collection

From all participants, hair specimens (about 1 g) were taken from the points of the nape near the hair skin by cutting with steel scissors (dyed hair not included in the study).

2.2. Measurement of Zn, Pb, Cd, Cr metal levels in hair tissue

Hair specimens taken were mixed with a mechanical shaker in a solution prepared by pure water containing 1% Triton x 100. Pure water inside was decanted and separated and then, rinsed with acetone for 10 min. The process of washing with acetone was repeated four times, and the specimens washed once more with pure water were dried overnight in an incubator at 55°C (Rahman et al. 2000:836).

From each washed and dried hair specimen, 0,2000±0,0002 g was weighed and 1 mL of concentrated HNO_3 in analytical purity was added and it was expected to be digested for eight hours. 10 mL of ultra-pure water was then, added to the specimen and stored at -20°C until measurement. The Zn, Pb, Cd, and Cr metal levels were determined using different commercial standard solutions for the element combined with an argon gas by inductively matched plasma optical emission spectrometry (ICP-OES, Thermo ICAP 6300 DUO Scientific) instrument (Table 1) (Rao et al. 2002:1334).

Table 1. ICP-OES: operating conditions and selected emission lines

Variable	
RF Power (KW)	0.95
Nebulizer gas flow ($l.min^{-1}$)	0.65
Auxiliary gas flow ($l.min^{-1}$)	0.50
Gas pressure (bar)	5.5-6
Low WL range	Axial: 5 WL Radial:5 WL
High WL range	Axial: 3 WL Radial: 3WL
Number of replicates	2
Read time (s)	26
Pump speed (rpm)	50
Cone	Zn
Emission lines (nm)	Zn: 213.56 Pb: 220.35 Cd: 228.80 Cr: 283.50

KW, kilowatts; RF, radio frequency; l, liter; min, minute; bar, bar; WL, waterless; s, second; rpm, cycle / minute; nm, nanometer.

2.3. Measurement of Zn, Pb, Cd, Cr metal levels in blood serum

The concentrations of Zn, Pb, Cd, and Cr in the serum specimens were measured using inductively matched plasma optical emission spectrometry (ICP-OES, Thermo ICAP 6300 DOU Scientific) and commercially available Merck branded standard solutions. Chemical standard mixtures were obtained by preparing stock solutions at varying concentrations for each metal element (Tascılar et al. 2011:189).

2.4. Measurement of serum reduced glutathione

The GSH activity was measured spectrophotometrically at 412 nm by a GSH disulfide reductase recycling method at room temperature (Tietz 1969:504). The reference rate was established using a freshly prepared GSH standard (30 mmol). The results were recorded in µmol.

2.5. Statistical Analysis

Statistical analysis was performed using the SPSS version 22.0 software (IBM Corp., Armonk, NY, USA). Descriptive data were expressed in mean ± standard deviation (SD) using the Microsoft Excel software (MS Excel, Microsoft Inc., Redmond, WA, USA). The Student's t-test was used to analyze the significant differences between the groups.

3. FINDINGS

The mean age of the research and control groups was 40.70±4.3 and 41.32±2.3 years, respectively. The body mass index (BMI) of the research and control groups was 22.56±1.70 kg/m^2 and 23.67±2.53 kg/m^2, respectively.

Table 2 shows the mean±standard deviation values of Zn, Pb, Cd, Cr metals measured in the hair specimens of the research and control groups and the level significance (p value) between the groups.

Table 2. Levels of Zn, Pb, Cd and Cr elements in hair specimens in research and control groups

	Petrol station workers (N=42)	Control group (N=25)	p
Zn (mg/g)	2.7500±1.281	2.0680±0.338	0.002
Pb(mg/g)	0.0218±0.017	0.0231±0.028	0.838
Cd (mg/g)	0.0069±0.005	0.0027±0.006	0.0001
Cr(mg/g)	0.0402±0.021	0.0061±0.003	0.0001

	Petrol station workers >40 age (N=12)	Petrol station workers <40 age (N=30)	p	Petrol station workers >30 age (N=23)	Petrol station workers <30 age (N=19)	p
Zn(mg/g)	2.6410± 0.854	2.7930± 1.427	0.674	2.5770± 0.842	2.9600± 1.668	0.003
Pb(mg/g)	0.0353± 0.021	0.0164± 0.011	0.011	0.0268± 0.019	0.0157± 0.0112	0.024
Cd(mg/g)	0.0096± 0.007	0.0058± 0.004	0.105	0.0077± 0.006	0.0059± 0.004	0.109
Cr(mg/g)	0.0443± 0.026	0.0386± 0.020	0.501	0.0409± 0.023	0.0393± 0.020	0.645

Zn, zinc; Pb, lead; Cd, cadmium; Cr, chromium; p, significance difference.

When the heavy metal levels in hair specimens were compared between the research and control groups, Zn, Cd and Cr metal levels of workers employed in petrol stations were found to be significantly higher than the control group ($p<0.05$) (Table 2). Although the value of Pb in the hair specimens of workers employed in petrol stations were slightly lower than the control group, there was no statistically significant difference ($p>0.05$). Pb, Cd and Cr metal levels were found to be higher in individuals over 40 years of age than those of under 30 years of age in the research group (long term exposure); however only Pb metal level differs significantly (Table 2). This indicates metal exposure due to increased term of employment.

Table 3. Serum levels of Zn, Pb, Cd and Cr elements in research and control groups

	Petrol station workers (N=42)	Control group (N=25)	p
Zn (mg/L)	0.7323±0.159	0.8034±0.118	0.041
Pb (mg/L)	0.0340±0.016	0.0292±0.013	0.196
Cd (mg/L)	0.0091±0.001	0.0093± 0.0007	0.364
Cr (mg/L)	0.1072±0.045	0.1409±0.010	0.0001

	Petrol station worker >40 age (N=12)	Petrol station worker <40 age (N=30)	p	Petrol Station workers >30 (N=23)	Petrol Station worker <30 (N=19)	p
Zn(mg/L)	0.7636± 0.251	0.7198± 0.107	0.569	0.7260± 0.105	0.7400± 0.105	0.770
Pb(mg/L)	0.0434± 0.192	0.0302± 0.013	0.046	0.0383± 0.017	0.0287± 0.014	0.055
Cd(mg/L)	0.0101± 0.001	0.0086± 0.001	0.002	0.0098± 0.001	0.0082± 0.001	0.0001
Cr(mg/L)	0.1250± 0.049	0.1001± 0.044	0.138	0.1183± 0.044	0.939± 0.044	0.085

Zn, zinc; Pb, lead; Cd, cadmium; Cr, chromium; p, significance difference.

The levels of Pb metal in serum samples of workers employed in petrol stations were higher than the control group (Table 3); however, the difference due to Zn and Cr levels was statistically significant ($p<0.05$). In addition, all four metal levels were higher in the research group of workers over age 40 than those of under 40 years of age (short term exposure), whereas only Pb and Cd metal exposures were statistically significant

(p<0.05). Again, this situation parallels both individuals over 30 and under 30 years of age in the research group other than metal level of Zn (Table 3) due to term of employment (Al-Rudainy 2010:208, WHO 2007).

Table 4. Serum levels of GSH in research and control groups

	Petrol station workers (N=42)		Control group (N=25)	p		
GSH(µmol)	10.81±2.09		10.44±1.70	0.431		
	Petrol station worker >40 age (N=12)	Petrol station workers <40 age (N=30)	p	Petrol station workers >30 age (N=23)	Petrol station worker< 30 age (N=19	p
GSH(µmol)	9.625± 1.45	11.29± 2.14	0.007	10.36± 1.70	11.36± 2.43	0.143

GSH, glutathione; p, significance difference.

The serum reduced GSH levels of petrol stations workers were lower than the control group due to metal exposure, but there was no significant difference (p>0.05). In addition, serum reduced GSH enzyme level of stations workers over age 40 were lower than activities of workers under age 40, and reached statistical significance (p<0.05) (Table 4). Although, the serum reduced GSH enzyme level of stations workers over 30 years was lower than those under 30 years of age, it was not statistically significant indicating minimum oxidative stress formation (p>0.05) (Table 4).

Heavy metals can be directly harmful to public health by entering the body through inhalation, dermal contact, dust and soil (Liu et al. 2007:209).

Human hair has been used extensively in recent years to observe metal toxicity, evaluate risk for human health, and determine the level of environmental exposure (Druyan et al. 1998:184). Metabolically inactive hair tissue is less sensitive to the intake of heavy metals and is therefore a useful biological indicator that characterizes long-term exposure in measuring metal contamination. In contrast, the passage of heavy metal atoms contained in petroleum products through the respiratory tract into the lung and then diffusion through the blood demonstrates short-term (several months) metal exposure (Estaban and Castano 2009:440).

In our research study, the mean amount of Zn in the hair specimens of the research group was found to be 2.7500±1.281 mg/g and 2.0680±0.338 mg/g in the control group, indicating a significant difference (p<0.05), and

these results are consistent with previous studies conducted in Baghdad and Beirut (Jamil et al. 1987:99, Nuwayhid et al. 2011:132). Similarly, in our research study, the mean amount of Zn in the serum specimens of the research group was found to be 0.7323±0.159 mg/L and 0.8034±0.118 mg/L in the control group, indicating a significant difference ($p<0.05$), and these results are consistent with Al-Faisal, Hussein and Abdul Kaleg (2010) (Al-Faisal et al. 2010:88).

In the present study, the mean hair and serum Pb levels of the research group were found to be approximate quantities with the control group and it did not reach statistical significance ($p<0.05$) due to the use of unleaded fuel-95 in the petroleum stations included in the research (Ogunseitan and Smith 2007:32).

The mean hair Cd levels was found to be higher than the control group with 0.0069±0.005 mg/g and 0.0027±0.006 mg/g and it reached statistical significance ($p<0.01$). El-Ghazaly et al. (2016) found that the amount of Cd metal in the liver tissue was significantly higher ($p<0.01$) than the control group in the oil-90 exposed albino rats, which is a kind of petroleum product in Egypt and it is consistent with our results (El-Ghazaly et al. 2016:36).

The level of Cr metal in hair tissue of the research group was significantly higher than the control group ($p<0.05$) which indicates a prolonged exposure to Cr metal in petroleum products (Mustafa et al. 2015:1350).

Due to an increased term of employment, the amount of Cd metal inhaled increased, leading to increased Cd serum concentrations (Table 3). Although similar results were obtained for serum Zn, Pb, and Cr metal amounts and only serum Pb and Cr reached statistical significance ($p<0.05$) and these results are consistent with the findings of Ahmed et al. (2013) (Ahmed et al. 2013:67).

In this study, serum reduced GSH levels was lower in the research group than the controls although the GSH level did not reach statistical significance ($p>0.05$). In 2017, Xia et al. conducted a study including workers working at a petroleum products filling station and found that mean serum GSH level was significantly lower ($p<0.05$) than the control group (Xia et al. 2017:175). In addition, serum GSH level of station workers over age 40 were found to be lower than workers under age 30 and under age 40; again serum GSH level of healthy control group individuals over age 40 were found to be lower than individuals under age 30 and under age 40, and therefore, GSH level decreased by increasing lifespan (Al-Faisal et al. 2010:88).

It can be assumed that the GSH activity of the research group decreased, caused by increased levels of Zn, Pb, Cr and Cd metal atoms, which were taken up by the inhalation of the petroleum products into the cell, to bind to the GSH -SH group, reducing their antioxidant capacity and activity. Since petroleum products contain some particles and volatile organic substances, petroleum workers are chronically exposed to these substances through inhalation (Vedal et al. 2019) and these petroleum compounds increase oxidative stress and inflammation (Vedal et al. 2013, Singaraju et al. 2012:2).

4. CONCLUSIONS

In conclusion, our study results showed that the workers working at a petroleum products filling station were exposed to toxicity of Cd, Pb metals and Zn and Cr heavy metals during unleaded fuel-95, diesel fuel, and liquid petroleum gas filling and the reduced GSH enzyme levels reduced consequently. For this reason, prompt necessary and extensive health precautions should be taken.

Given the fact that the term of employment have increasing with increased heavy metal exposure. Again, due to increased lifespan, the antioxidant defense mechanisms tend to decrease. In addition to abovementioned subjects, investigating amount of heavy metals content of petroleum products and the structure of the marker substances added to the diesel will be useful.

References

Al-Fartosy Adnan JM, Sanaa K. Shanan and Nadhum A. Awad. (2017) Biochemical Study of the Effects of Some Heavy Metals on Oxidant / Antioxidant Status in Gasoline Station Workers / Basra-Iraq. International Journal of Scientific and Research Publications (IJSRP) 7(2): 83-93

Ahmed, M.K., Awad Kundu, A., Al-Mamun, M.H., Sarkar, D.K., Akter, M.S. and Khan, M.S. (2013) Chromium (VI) induced acute toxicity and genotoxicity in freshwater stinging catfish, Heteropneustes fossilis. Ecotoxicology and Environmental Safety, 92: 64-70.

Al-Faisal, A.H.M., Hussein, A.M. and Abdul Kaleg, A.R. (2010) Estimation of DNA Damages; Cytotoxicity and Antioxidant Status of Heavy Metals and Benzene among Petrol Workers in Baghdad-Iraq." IJPS, 6(1): 85-94.

Al-Rudainy, L.A. (2010). Blood lead level among fuel station workers. Oman Medical Research, 25(3): 208-211.

Asri FÖ, Sönmez S (2006) Ağır metal toksisitesinin bitki metabolizması üzerine etkileri. Derim 23(2): 36-45

ATSDR (2005) Toxicological Profile for Zinc, Agency for Toxic Substances and Disease Registry. US Public Health Service

Ciftçi Y, Işık MA, Akerli T, Yeşilova Ç (2008). Van gölü havzasının çevre jeolojisi. Geological Engineering Journal 32(22): 45-77

Commision TE (1967) Council Directive 67/548/EECof 18 August 1967 on the approximation of the laws, regulations and administrative provisions relating to the classification, packaging and labelling of dangerous substances. Off J Eur Communities 96: 1-98

Dietz R, Outridge PM, Hobson KA (2009) Anthropogenic contributions to mercury levels in present-day Arctic animals—a review. Sci Total Environ 407: 6120–6131

Druyan ME, Bass D, Puchyr R, Urek K, Quig D, Harmon E, Marquardt W (1998) Determination of reference ranges for elements in human scalp hair. Biol Trace Elem Res. 62: 183–187

El-Ghazaly, N., Ali, A., Dekinesh, S., Sedky, A. and Kabeil, S. (2016) Hepatotoxicity of Gasoline as an Environmental Pollutant on Albino Mice. Athens Journal of Sciences, 3(1): 31-44.

Esteban M, Castano A (2009) Non-invasive matrices in human biomonitoring: a review. Environ. Int. 35: 438–449

Grevatt PC (1998) Toxicological review of hexavalent chromium. Support of summary information on the integrated risk information system (IRIS). US Enviromental Protection Agency, Washington DC

Jaishankar M, Tseten T, Anbalagan N, Mathew BB, Beeregowda KN (2014). Toxicity, mechanism and health effects of some heavy metals. Interdiscip Toxicol. 7(2): 60-72

Jarup L (2003). Hazards of heavy metal contamination. Br Med Bull 68: 167-182

Jamil, H., Dhia, J.A., Saad, I.A. & Qasim, IV. (1987) Lead absorption in petrol filling station workers in Baghdad city. Journal of the Faculty of Medicine Baghdad, 29(1): 95-102.

Liu WX, Shen LF, Liu JW, Wang YW, Li SR (2007) Uptake of toxic heavy metals by rice (Oryza sativa L.) cultivated in the agricultural soils near Zhengzhou City, People's Republic of China. Bull. Environ. Contam. Toxicol, 79: 209–213

Luckett BG, Su LJ, Rood JC, Fontham ET (2012). Cadmium exposure and pancreatic cancer in south Louisiana. J Environ Public Health 2012:180-186

Mustafa, A.D., Juahir, H., Yunus, K., Amran, M.A., Hasnam, C.N.C., Azaman, F., Abidin, I.Z., Azmee, S.H. and Sulaiman, N.H. (2015) Oil spill related heavy metal: a review. Malaysian Journal of Analytical Sciences, 19(6): 1348-1360.

Nuwayhid, I., McPhaul, K., Bu-Khuzam, R., Duh, S.H., Christenson, R.H. and Keogh, J.P. (2011) Determinants of elevated blood lead levels

among working men in Greater Beirut. Journal of Medicine Libanese (J Med Liban), 49(3): 132-139.
Ogunseitan, O.A. and Smith, T. (2007) The cost of environmental lead (Pb) poisoning in Nigeria. African Journal of Environmental Science and Technology, 1(2):027-036.
Parcell S (2002). Sulfur in human nutrition and applications in medicine. Altern Med Rev 7: 22-44
Rahman, L., Corns, W.T., Bryce, D.W. and Stockwell, P.B. (2000) Determination of mercury, selenium, bismuth, arsenic and antimony in human hair by microwave digestion atomic fluorescence spectrometry. Talanta, 52: 833–843.
Rao, K.S., Balaji, T., Rao, T.P., Babu, Y. and Naidu, G.R.K. (2002) Determination of iron, cobalt, nickel, manganese, zinc, copper, cadmium and lead in human hair by inductively coupled plasma atomic emission spectrometry. Spectrochimica Acta Part B 57:1333-1338.
Singaraju, M., Singaraju, S., Parwani, R. and Wanjari, S.P. (2012) Cytogenetic biomonitoring in petrol station attendants: a micronucleus study. Journal of Cytology, 29 (1): 1–5.
Tascilar, M.E., Ozgen, I.T., Abaci, A., Serdar, M. and Aykut, O. (2011) Trace elements in obese Turkish children. Biological Trace Elements Research 143(1): 188-195.
Tietz, F. (1969) Enzymic method for quantitative determination of nanogram amounts of total and oxidized glutathione: applications to mammalian blood and other tissues. Analytical Biochemistry, 27: 502-522.
Waseem A, Arshad J, Iqbal F, Sajjad A, Mehmood Z, Murtaza G (2014) Pollution status of Pakistan: a retrospective review on heavy metal contamination of water, soil and vegetables. Biomed Res. Int. 813206: 1-29
WHO (World Health Organization). Health risks of heavy metals from long range trans-boundary air pollution. World Health Organization Regional Office for Europe. Copenhagen, Denmark. pp. 40–45. 2007. Available at: http://www.euro.who.int/_data/assets/pdf_file/0007/78649/E91044.pdf Accessed October 3, 2019
Wong SL, Lye EJ (2008). Lead, mercury and cadmium levels in Canadians. Health Rep 19(4): 31-36
Xia, B., Chen, K., Lv, Y., Huang, D., Liu, J., Liang, G., Zhang, L., Wang, F., Su, C., Zou, Y. and Yang, X. (2017) Increased oxidative stress and plasma Hsp70 levels among gasoline filling station attendants. Toxicology and Industrial Health, 33(2): 171-181.
Vedal, S., Campen, M.J. and McDonald, J.D. National Particle Component Toxicity (NPACT) initiative report on cardiovascular effects.

Research Report Health Effective Institue, 178: 5–8. Research Report 178. Boston, MA. 2013. Available at: http://www.healtheffects.org/system/files/RR178-Vedal.pdf Accessed October 3, 2019.

CHAPTER III

ON PROLONGATIONS OF METALLIC STRUCTURES TO TANGENT BUNDLES OF ORDER TWO

Assoc. Prof. Dr. Mustafa ÖZKAN

Gazi University, Ankara, Turkey, e-mail: ozkanm@gazi.edu.tr
Orcid No: 0000-0002-5883-2294

Ceyda AYAZ

Gazi University, Ankara, Turkey, e-mail: ceydaayazz93@gmail.com
Orcid No: 0000-0003-0384-7031

1. Introduction

The method of lift has an important role in modern differentiable geometry. Let $\mathcal{M}$ be an n-dim differentiable manifold of class C^∞. Extension of fundamental differentiable elements like function, vector field, 1-form, connection, metric and tensor field on $\mathcal{M}$ to other manifolds is crucial in terms of explaining relations between these manifolds. This process is provided by prolonging the differentiable elements on $\mathcal{M}$ to the other manifolds using their lifts. Excluding the manifolds that are diffeomorph to the $\mathcal{M}$, we can list the manifolds that have the closest relationship with the $\mathcal{M}$ manifold as $T\mathcal{M}, T_2\mathcal{M}, TT\mathcal{M}$…. Lifts of structures on any manifold M to its tangent bundle of order two were introduced and studied by several authors, see (Das, 1993; Keçilioğlu, 2010; Mathai, 1975; Özkan et al., 2015; Özkan et al., 2017; Yano and Ishihara, 1973).

The golden ratio is known to everyone and it has many application areas such as architecture, painting, design and music studies. The golden ratio has also become an inspiration for mathematicians. Hreţcanu, in (Hreţcanu, 2007), defined the golden structure on a differentiable manifold $\mathcal{M}$ with the help of a tensor field Φ of type $(1,1)$ on $\mathcal{M}$ satisfying $Q(X) = X^2 - X - I$. Then, the geometry of this structure on $\mathcal{M}$ was examined by (Crasmareanu and Hreţcanu, 2008). Golden structures were studied by various authors (Beldjilali, 2019, 2020; Erdoğan, 2019; Gezer et al. 2013; Gezer and Karaman, 2016; Özkan, 2014; Savas, 2017). Özkan and Peltek,

This work is derived from the master's thesis by Ceyda AYAZ.

in (Özkan and Peltek, 2013, 2016), have defined a silver structure with the structure polynomial $Q(X) = X^2 - 2X - I$, on a differentiable manifold. Moreover, Özkan and Yılmaz, in (Özkan and Yılmaz, 2015), have investigated a bronze structure with the structure polynomial $Q(X) = X^2 - X - 2I$, on a differentiable manifold.

Spinadel, in (Spinadel, 1997), described the metallic ratio, which is an expansion of the golden ratio. The metallic ratio family includes gold, silver, bronze, copper and other structures.

The positive root of the equation

$$x^2 - ax - b = 0$$

is called members of the metallic means family for positive integers a and b. This root is denoted by

$$\rho_{a,b} = \frac{a+\sqrt{a^2+4b}}{2}$$

and it is known as metallic ratio (Hreţcanu and Crasmareanu, 2013; Spinadel, 1997, 1999, 2000)

Hreţcanu and Crasmareanu, in (Hreţcanu and Crasmareanu, 2013), defined the metallic structure by a tensor field of type $(1,1)$ satisfying $Q(X) = X^2 - aX - bI$. This structure was a generalization of the golden structure. Yılmaz, in (Yılmaz, 2016), and Özkan and Yılmaz, in (Özkan and Yılmaz, 2018), investigated the geometry of this metallic structure. Özkan and Uz, in (Özkan and Uz, 2016), worked on prolongations of metallic structures to the tangent bundles. Metallic structures were studied by various authors (Akyol, 2019; Erdoğam et al., 2019; Gezer and Karaman, 2015).

In this study, first of all, in order to understand better the next chapters, some definitions and theorems are summarized, in the literature. Then, the metallic structures on a differentiable manifold have been prolonged to the tangent bundle of order two of this manifold through the second lift. Next, some essential definitions and theorems about the integrability and parallelism of this metallic structure on the tangent bundle of order two were given. Finally, the metric, which was defined on the prolonged metallic structure, and its properties were examined.

Let us denote by $F(\mathcal{M})$ the algebra of C^∞-reel functions on $\mathcal{M}$, $\Gamma(\mathcal{M}) = \chi(\mathcal{M}) = \Im_0^1(\mathcal{M})$ the Lie algebra of vector fields on $\mathcal{M}$, $\Im_s^r(\mathcal{M})$ the $F(\mathcal{M})$-module of tensor fields of (r,s)-type on $\mathcal{M}$.Throughout this paper, all manifolds, bundles, tensor fields, and connections are assumed to be of C^∞.

Definition 1.1. Let $\mathcal{J}$ be a tensor field of type $(1,1)$ on $\mathcal{M}$. $\mathcal{J}$ which satisfies the equation

$$\mathcal{J}^2 - a\mathcal{J} - bI = 0 \tag{1}$$

is called a metallic structure on $\mathcal{M}$ where a, b are positive integers and I is the identity operator on $\chi(\mathcal{M})$. The pair $(\mathcal{M}, \mathcal{J})$ is a metallic manifold (Hreţcanu and Crasmareanu, 2013; Yılmaz, 2016; Özkan and Yılmaz, 2018).

Theorem 1.2. If P is an almost product structure on manifold $\mathcal{M}$ then

$$\mathcal{J} = \frac{a}{2}I + \left(\frac{2\rho_{a,b}-a}{2}\right)P \tag{2}$$

is metallic structure on $\mathcal{M}$. Conversely, if $\mathcal{J}$ is a metallic structure on $\mathcal{M}$ then

$$P = \frac{2}{2\rho_{a,b}-a}\mathcal{J} - \frac{a}{2\rho_{a,b}-a}I. \tag{3}$$

are almost product structures on $\mathcal{M}$ (Hreţcanu and Crasmareanu, 2013; Yılmaz, 2016; Özkan and Yılmaz, 2018).

Let the operators k and l be defined as (Hreţcanu and Crasmareanu, 2013; Yılmaz 2016; Özkan and Yılmaz, 2018)

$$k = \frac{1}{2\rho_{a,b}-a}\mathcal{J} - \frac{a-\rho_{a,b}}{2\rho_{a,b}-a}I,\ l = -\frac{1}{2\rho_{a,b}-a}\mathcal{J} + \frac{\rho_{a,b}}{2\rho_{a,b}-a}I \tag{4}$$

where $\rho_{a,b} = \frac{a+\sqrt{a^2+4b}}{2}$. Then we get

$$k + l = I,\ kl = lk = 0,\ (k)^2 = k,\ (l)^2 = l, \tag{5}$$

$$\mathcal{J}k = k\mathcal{J} = \rho_{a,b}k,\ \mathcal{J}l = l\mathcal{J} = (a - \rho_{a,b})l. \tag{6}$$

Thus K and L are two complementary distributions on $(\mathcal{M}, \mathcal{J})$ metallic manifold corresponding $\rho_{a,b}$ and $a - \rho_{a,b}$, respectively. The corresponding projection operators of K and L are denoted by k and l respectively (Hreţcanu and Crasmareanu, 2013; Yılmaz 2016; Özkan and Yılmaz, 2018).

2. Prolongations of metallic structure to tangent bundle of order two

Let $\mathcal{M}$ be an n −dim differentiable manifold of class C^∞. We introduce an equivalence relation $\sim$ in the set of all differentiable mappings. We denote these mappings by $C(\mathcal{M})$. If the mappings $G: \mathbb{R} \to \mathcal{M}$ and $H: \mathbb{R} \to \mathcal{M}$ satisfy the following conditions

$$G(0) = H(0),\ \frac{dG^i(0)}{dt} = \frac{dH^i(0)}{dt},\ \frac{d^2G^i(0)}{dt^2} = \frac{d^2H^i(0)}{dt^2},$$

where G and H are indicated respectively by $x^i = G^i(t)$ and $x^i = H^i(t)$ with respect to local coordinates x^i in a coordinate neighborhood of $\{V, x^i\}$ containing the point $G(0) = H(0) = p \in V$. In this case, we call that the mapping G is equivalent to H and denoted by $G \sim H$. Each equivalence relation is called 2-jet of $\mathcal{M}$ and shown by $j_p^2(G)$. The set of all $2-$jets of $\mathcal{M}$ is called the tangent bundle of order 2 and denoted by $T_2(\mathcal{M})$, and $\pi_2: T_2(\mathcal{M}) \to \mathcal{M}$ is the bundle projection of $T_2(\mathcal{M})$ to $\mathcal{M}$. Then $T_2(\mathcal{M})$ is also a differentiable manifold of class C^∞ and its dim is $3n$. The tangent bundle $T_1(\mathcal{M})$ of order 1 is the tangent bundle $T\mathcal{M}$ over $\mathcal{M}$ and $\pi_1: T\mathcal{M} \to \mathcal{M}$ is the bundle projection of $T\mathcal{M}$ to $\mathcal{M}$. Then $T_1(\mathcal{M})$ is also $2n$-dim a differentiable manifold of class C^∞. If π_{12} is the mapping $\pi_{12}: T_2(\mathcal{M}) \to T\mathcal{M}$ then $T_2(\mathcal{M})$ has a bundle structure over $T\mathcal{M}$ with projection π_{12} (Yano and Ishihara, 1968; Yano and Ishihara, 1973).

Let $\{V, x^i\}$ be a coordinate neighborhood of $\mathcal{M}$ and $G: \mathbb{R} \to \mathcal{M}$ be differentiable map such that $G(0) = p$. The local coordinates of $T_2\mathcal{M}$ are indicated by the set (x^i, y^i, z^i) in the open set $\pi_2^{-1}(V)$ of $T_2(\mathcal{M})$ where x^i is the coordinates of p in V, y^i, z^i are defined respectively by $y^i = \frac{dG^i(0)}{dt}$, $z^i = \frac{1}{2}\frac{d^2G^i(0)}{dt^2}$ where $x^i = G^i(t)$ with the point p. (x^i, y^i, z^i) is called the induced coordinates in $\pi_2^{-1}(V)$ (Yano and Ishihara, 1968; Yano and Ishihara, 1973).

Let $\mathcal{J} \in \Im_1^1(\mathcal{M})$ and $\mathcal{J}$ have local components $\mathcal{J}_j^i$ in a coordinate neighborhood $\{V, x^i\}$ of $\mathcal{M}$. Then the second lift $\mathcal{J}^{II}$ of $\mathcal{J}$ in $T_2(\mathcal{M})$ will have the components of the form (Yano and Ishihara, 1968; Yano and Ishihara, 1973)

$$\mathcal{J}^{II} = \mathcal{J}_j^i\left(\frac{\partial}{\partial x^i} \otimes dx^j + \frac{\partial}{\partial y^i} \otimes dy^j + \frac{\partial}{\partial z^i} \otimes dz^j\right)$$
$$+ y^h \partial_h \mathcal{J}_j^i \left(\frac{\partial}{\partial y^i} \otimes dx^j + \frac{\partial}{\partial z^i} \otimes dy^j\right)$$
$$+ \left(z^h \partial_h \mathcal{J}_j^i + \frac{1}{2} y^h y^t \partial_h \partial_t \mathcal{J}_j^i\right) \frac{\partial}{\partial z^i} \otimes dx^j$$

with respect to the induced coordinates (x^i, y^i, z^i) in $T_2(\mathcal{M})$.

For any $\mathcal{J}, \Phi \in \Im_1^1(\mathcal{M})$, we have (Yano and Ishihara, 1968; Yano and Ishihara, 1973)

$$(\mathcal{J}\Phi)^{II} = \mathcal{J}^{II}\Phi^{II}. \tag{7}$$

Replacing Φ by $\mathcal{J}$ in (7), we obtain

$$(\mathcal{J}^2)^{II} = (\mathcal{J}^{II})^2. \tag{8}$$

Taking the second lift on both sides of equation (1), we have $(\mathcal{J}^2 - a\mathcal{J} - bI)^{II} = 0$. Using (8) and $I^{II} = I$, we obtain

$$(\mathcal{J}^{II})^2 - a\mathcal{J}^{II} - bI = 0. \tag{9}$$

Thus we have the following proposition.

Proposition 2.1. Let $\mathcal{J}$ be an element of $\Im_1^1(\mathcal{M})$. Then the second lift $\mathcal{J}^{II}$ of $\mathcal{J}$ is a metallic structure on $T_2(\mathcal{M})$ if and only if $\mathcal{J}$ is metallic structure on $\mathcal{M}$.

Proposition 2.2. (*i*) If $\mathcal{J}$ is a metallic structure on $\mathcal{M}$, then the metallic structure $\mathcal{J}^{II}$ an isomorphism on the tangent space of the tangent manifold $T_q(T_2(\mathcal{M}))$ for $\forall\, q \in T_2(\mathcal{M})$.

(*ii*) $\mathcal{J}^{II}$ is invertible and its inverse $(\mathcal{J}^{II})^{-1} = \bar{\mathcal{J}}^{II}$ satisfies

$$(\bar{\mathcal{J}}^{II})^2 + \tfrac{a}{b}\bar{\mathcal{J}}^{II} - \tfrac{1}{b}I = 0.$$

Remark 2.3. Let P and C be an almost product and an almost complex structure on $\mathcal{M}$, respectively. Then P^{II} and C^{II} are an almost product and an almost complex structure, and $-P^{II}$ and $-C^{II}$ are also an almost product and an almost complex structure on $T_2(\mathcal{M})$, respectively.

We can give a similar relationship for metallic structures. From (Yılmaz, 2016; Özkan and Yılmaz, 2018) we can give following proposition.

Proposition 2.4. If $\mathcal{J}$ is a metallic structure, then $\tilde{\mathcal{J}}^{II} = aI - \mathcal{J}^{II}$ is also a metallic structure on $T_2(\mathcal{M})$.

Taking the second lift on both sides of equation (2), (3) and taking account of Remark 2.3., we have the following theorem.

Theorem 2.5. Let P be an almost product structure on $\mathcal{M}$. Every almost product structure P^{II} induces a metallic structure on $T_2(\mathcal{M})$ as follows:

$$\mathcal{J}^{II} = \tfrac{a}{2}I + \left(\tfrac{2\rho_{a,b}-a}{2}\right)P^{II}. \tag{10}$$

Conversely, let $\mathcal{J}$ be a metallic structure on $\mathcal{M}$. Every metallic structure $\mathcal{J}^{II}$ yields an almost product structure on $T_2(\mathcal{M})$

$$P^{II} = \frac{2}{2\rho_{a,b}-a}\mathcal{J}^{II} - \frac{a}{2\rho_{a,b}-a}I. \tag{11}$$

Definition 2.6. Let $(\mathcal{M}, T)$ be an almost tangent manifold. Then

$$\mathcal{J}_t^{II} = \frac{a}{2} I + \left(\frac{2\rho_{a,b}-a}{2}\right) T^{II}$$

is called a tangent metallic structure on $T_2(\mathcal{M})$.

The polynomial equation satisfied by $\mathcal{J}_t^{II}$ is

$$(\mathcal{J}_t^{II})^2 - a\mathcal{J}_t^{II} + \frac{a^2}{4} I = 0.$$

Definition 2.7. Let $(\mathcal{M}, C)$ be an almost complex manifold. Then

$$\mathcal{J}_c^{II} = \frac{a}{2} I + \left(\frac{2\rho_{a,b}-a}{2}\right) C^{II}$$

is called a complex metallic structure on $T_2(\mathcal{M})$.

The $\mathcal{J}_c^{II}$ structure verifies the following equation:

$$(\mathcal{J}_c^{II})^2 - a\mathcal{J}_c^{II} + \frac{a^2+2b}{2} I = 0.$$

From (Özkan and Yılmaz, 2018), we can give following example.

Example 2.8. From (10), we get

$$\mathcal{J}_{F^{II}} = \frac{a}{2} I + \left(\frac{2\rho_{a,b}-a}{2}\right) F^{II},\ \mathcal{J}_{T^{II}} = \frac{a}{2} I + \left(\frac{2\rho_{a,b}-a}{2}\right) T^{II},$$

$$\mathcal{J}_{K^{II}} = \frac{a}{2} I + \left(\frac{2\rho_{a,b}-a}{2}\right) K^{II}$$

where $F, T \in \Im_1^1(\mathcal{M})$ and $K = T \circ F$. Hence we obtain

$$\sqrt{a^2+4b}\,\mathcal{J}_{F^{II}} = 2\mathcal{J}_{T^{II}}\mathcal{J}_{F^{II}} - a\mathcal{J}_{T^{II}} - a\mathcal{J}_{F^{II}} + \rho_{a,b}^2 I - bI$$

where $\rho_{a,b} = \frac{a+\sqrt{a^2+4b}}{2}$ is the metallic ratio and the $\left(\mathcal{J}_{F^{II}}, \mathcal{J}_{T^{II}}, \mathcal{J}_{F^{II}}\right)$ is:

(*i*) An almost hyperproduct (ahp)-structure in $T_2(\mathcal{M})$ if and only if $(\mathcal{J}_F, \mathcal{J}_T, \mathcal{J}_K)$ is (ahp)-structure on $\mathcal{M}$.

(*ii*) An almost biproduct complex (abpc)-structure in $T_2(\mathcal{M})$ if and only if $(\mathcal{J}_F, \mathcal{J}_T, \mathcal{J}_K)$ is (abpc)-structure on $\mathcal{M}$.

(*iii*) An almost product bicomplex (apbc)-structure in $T_2(\mathcal{M})$ if and only if $(\mathcal{J}_F, \mathcal{J}_T, \mathcal{J}_K)$ is (apbc)-structure on $\mathcal{M}$.

(*iv*) An almost hypercomplex (ahc)-structure in $T_2(\mathcal{M})$ if and only if $(\mathcal{J}_F, \mathcal{J}_T, \mathcal{J}_K)$ is (ahc)-structure on $\mathcal{M}$.

3. Integrability and parallelism of metallic structures in tangent bundle of order two

Let P, $\mathcal{J}$ are almost product and metallic structures on $\mathcal{M}$, respectively. Then the Nijenhuis tensor N_P of P and $N_{\mathcal{J}}$ of $\mathcal{J}$ are tensor fields of type

(1,2) given by (Hreţcanu and Crasmareanu, 2013; Yano. and Ishihara, 1973)

$$N_P(X,Y) = [PX,PY] - P[PX,Y] - P[X,PY] + P^2[X,Y],$$
$$N_{\mathcal{J}}(X,Y) = [\mathcal{J}X,\mathcal{J}Y] - \mathcal{J}[\mathcal{J}X,Y] - \mathcal{J}[X,\mathcal{J}Y] + \mathcal{J}^2[X,Y]. \quad (12)$$

for any $X,Y \in \chi(\mathcal{M})$, respectively.

For any $X,Y \in \chi(\mathcal{M})$ and

$$\mathcal{J} = \frac{a}{2}I + \left(\frac{2\rho_{a,b}-a}{2}\right)P,$$

the following relations are satisfied (Yılmaz 2016; Özkan and Yılmaz, 2018)

$$N_P(X,Y) = \frac{4}{(2\rho_{a,b}-a)^2}N_{\mathcal{J}}(X,Y). \quad (13)$$

For any $X,Y \in \chi(\mathcal{M})$ and $\mathcal{J} \in \Im_1^1(\mathcal{M})$, we have (Yano and Ishihara, 1973)

$$(X+Y)^{II} = X^{II} + Y^{II},$$
$$[X^{II},Y^{II}] = [X,Y]^{II}, \quad (14)$$
$$\Phi^{II}X^{II} = (\Phi X)^{II}.$$

From (4), (5), (6), (7) and (8), we give following proposition and remark.

Proposition 3.1. Let $\mathcal{J}^{II}$ be a metallic structure on $T_2(\mathcal{M})$. There exist on $T_2(\mathcal{M})$ two complementary distributions K^{II} and L^{II} corresponding to the projection operators

$$k^{II} = \frac{1}{2\rho_{a,b}-a}J^{II} - \frac{a-\rho_{a,b}}{2\rho_{a,b}-a}I,$$
$$l^{II} = -\frac{1}{2\rho_{a,b}-a}J^{II} + \frac{\rho_{a,b}}{2\rho_{a,b}-a}I. \quad (15)$$

Remark 3.2. The projection tensors k^{II} and l^{II} satisfies following:

$$k^{II} + l^{II} = I, \qquad k^{II}l^{II} = l^{II}k^{II} = 0, \quad (16)$$
$$(k^{II})^2 = k^{II}, \qquad (l^{II})^2 = l^{II},$$
$$\mathcal{J}^{II}k^{II} = k^{II}\mathcal{J}^{II} = \rho_{a,b}k^{II}, \quad (17)$$
$$\mathcal{J}^{II}l^{II} = l^{II}\mathcal{J}^{II} = (a-\rho_{a,b})l^{II}.$$

Hence the second lift k^{II} of k and l^{II} of l define complementary distributions K^{II} and L^{II} corresponding to these projections.

Let $N_{P^{II}}$, $N_{\Phi^{II}}$ be the Nijenhuis tensor of P^{II} and of Φ^{II} in $T_2(\mathcal{M})$, respectively. Then in view of (8), we have

$$N_{P^{II}}(X^{II},Y^{II}) = [P^{II}X^{II},P^{II}Y^{II}] - P^{II}[P^{II}X^{II},Y^{II}] - P^{II}[X^{II},P^{II}Y^{II}] + (P^2)^{II}[X^{II},Y^{II}], \quad (18)$$

$$N_{\mathcal{J}^{II}}(X^{II},Y^{II}) = [\mathcal{J}^{II}X^{II},\mathcal{J}^{II}Y^{II}] - \mathcal{J}^{II}[\mathcal{J}^{II}X^{II},Y^{II}] - \mathcal{J}^{II}[X^{II},\mathcal{J}^{II}Y^{II}] + (\mathcal{J}^{II})^2[X^{II},Y^{II}] \quad (19)$$

where $X, Y \in \chi(\mathcal{M})$.

Proposition 3.3. The second lift K^{II} of a distribution K in $T_2(\mathcal{M})$ is integrable if and only if K is integrable in $\mathcal{M}$.

Proof. The distribution K is integrable if and only if (Özkan and Yılmaz, 2018)

$$l[kX,kY] = 0 \quad (20)$$

for any $X, Y \in \chi(\mathcal{M})$.

Taking second lift on both sides of equation (20) and using (14), we get

$$l^{II}[k^{II}X^{II},k^{II}Y^{II}] = 0. \quad (21)$$

where $l^{II} = (I-k)^{II} = I - k^{II}$, is the projection tensor complementary to k^{II}. Thus the conditions (20) and (21) are equivalent. Hence the theorem is proved. □

Proposition 3.4. Let the distribution K be integrable in $\mathcal{M}$. Then the distribution K^{II} is integrable in $T_2(\mathcal{M})$, if and only if

$$l^{II}N_{\mathcal{J}^{II}}(k^{II}X^{II},k^{II}Y^{II}) = 0$$

for any $X, Y \in \chi(\mathcal{M})$,

Proof. The distribution K is integrable if and only if (Özkan and Yılmaz, 2018)

$$lN_{\mathcal{J}}(kX,kY) = 0$$

for any $X, Y \in \chi(\mathcal{M})$.

Taking account of the Nijenhuis tensor of $\mathcal{J}^{II}$, we obtain

$$N_{\mathcal{J}^{II}}(k^{II}X^{II},k^{II}Y^{II}) = [\mathcal{J}^{II}k^{II}X^{II},\mathcal{J}^{II}k^{II}Y^{II}] - \mathcal{J}^{II}[\mathcal{J}^{II}k^{II}X^{II},k^{II}Y^{II}] - \mathcal{J}^{II}[k^{II}X^{II},\mathcal{J}^{II}k^{II}Y^{II}]$$

$$+(\mathcal{J}^2)^{II}[k^{II}X^{II}, k^{II}Y^{II}] \tag{22}$$

Equation (22), with the help of (9) and (17) gives

$$N_{\mathcal{J}^{II}}(k^{II}X^{II}, k^{II}Y^{II}) = \big(a - 2\sigma_{a,b}\big)\mathcal{J}^{II}[k^{II}X^{II}, k^{II}Y^{II}]$$
$$+\big(2b + a\sigma_{a,b}\big)[k^{II}X^{II}, k^{II}Y^{II}].$$

Multiplying throughout by $\frac{1}{(2\sigma_{a,b}-a)^2} l^{II}$ and from (17), we get

$$\frac{1}{(2\sigma_{a,b}-a)^2} l^{II}\, N_{\mathcal{J}^{II}}(k^{II}X^{II}, k^{II}Y^{II}) = l^{II}[k^{II}X^{II}, k^{II}Y^{II}]$$
$$= \Big(lN_{\mathcal{J}}(kX, kY)\Big)^{II}$$

Using (21) (or $lN_{\mathcal{J}}(kX, kY) = 0$), we have

$$l^{II}N_{\mathcal{J}^{II}}(k^{II}X^{II}, k^{II}Y^{II}) = 0.$$ □

Proposition 3.5. The second lift L^{II} of a distribution L in $T_2(\mathcal{M})$ is integrable if and only if L is integrable in $\mathcal{M}$.

Proof. The distribution L is integrable if and only if (Özkan and Yılmaz, 2018)

$$k[lX, lY] = 0 \tag{23}$$

for any $X, Y \in \chi(\mathcal{M})$.

Taking second lift on both sides of equation (23) and using (1), we get

$$l^{II}[l^{II}X^{II}, l^{II}Y^{II}] = 0 \tag{24}$$

where $k^{II} = (I - l)^{II} = I - l^{II}$, is the projection tensor complementary to l^{II}. Thus the conditions (23) and (24) are equivalent. Hence the theorem is proved. □

Proposition 3.6. Let the distribution L be integrable in $\mathcal{M}$. Then the distribution L^{II} is integrable in $T_2(\mathcal{M})$ if and only if

$$k^{II}N_{\mathcal{J}^{II}}(l^{II}X^{II}, l^{II}Y^{II}) = 0$$

for any $X, Y \in \chi(\mathcal{M})$,

Proof. In (Özkan and Yılmaz, 2018), we know that the distribution L is integrable if and only if

$$kN_{\mathcal{J}}(lX, lY) = 0$$

for any $X, Y \in \chi(\mathcal{M})$.

Then in view of (12), we have

$$N_{\mathcal{J}^{II}}(l^{II}X^{II}, l^{II}Y^{II}) = [\mathcal{J}^{II}l^{II}X^{II}, \mathcal{J}^{II}l^{II}Y^{II}] - \mathcal{J}^{II}[\mathcal{J}^{II}l^{II}X^{II}, l^{II}Y^{II}]$$
$$-\mathcal{J}^{II}[l^{II}X^{II}, \mathcal{J}^{II}l^{II}Y^{II}]$$
$$+(\mathcal{J}^{2})^{II}[l^{II}X^{II}, l^{II}Y^{II}]. \qquad (25)$$

Equation (25), with the help of (9) and (17) gives

$$N_{\mathcal{J}^{II}}(l^{II}X^{II}, l^{II}Y^{II}) = \left(2\rho_{a,b} - a\right)\mathcal{J}^{II}[l^{II}X^{II}, l^{II}Y^{II}]$$
$$+\left(a^{2} + 2b - a\rho_{a,b}\right)[l^{II}X^{II}, l^{II}Y^{II}].$$

Multiplying throughout by $\frac{1}{\left(2\sigma_{a,b}-a\right)^{2}}k^{II}$ and from (17), we get

$$\frac{1}{\left(2\sigma_{a,b}-a\right)^{2}}k^{II}N_{\mathcal{J}^{II}}(l^{II}X^{II}, l^{II}Y^{II}) = k^{II}[l^{II}X^{II}, l^{II}Y^{II}]$$
$$= \left(kN_{\mathcal{J}}(lX, lY)\right)^{II}.$$

Using (24) (or $kN_{\mathcal{J}}(lX, lY) = 0$), we have

$$k^{II}N_{\mathcal{J}^{II}}(l^{II}X^{II}, l^{II}Y^{II}) = 0.$$ □

Proposition 3.7. For any $X, Y \in \chi(\mathcal{M})$ and $\mathcal{J}^{II} = \frac{a}{2}I + \left(\frac{2\rho_{a,b}-a}{2}\right)P^{II}$, the following relation between $N_{P^{II}}$ and $N_{\mathcal{J}^{II}}$ is satisfying

$$N_{P^{II}}(X^{II}, Y^{II}) = \frac{4}{\left(2\rho_{a,b}-a\right)^{2}}N_{\mathcal{J}^{II}}(X^{II}, Y^{II}).$$

Proof. In view of (11), (13), (14) and (18) we have

$$N_{P^{II}}(X^{II}, Y^{II}) = \left(N_{P}(X, Y)\right)^{II} = \left(\frac{4}{\left(2\rho_{a,b}-a\right)^{2}}N_{\mathcal{J}}(X, Y)\right)^{II}$$
$$= \frac{4}{\left(2\rho_{a,b}-a\right)^{2}}N_{\mathcal{J}^{II}}(X^{II}, Y^{II}).$$ □

Thus we can give the following proposition.

Proposition 3.8. Let P almost product structure on $\mathcal{M}$ and the second lifts $\mathcal{J}^{II}$ of $\mathcal{J}$ is metallic structures on $T_2(\mathcal{M})$. Then $\mathcal{J}^{II}$ is integrable on $T_2(\mathcal{M})$ if and only if P is integrable on $\mathcal{M}$.

Proposition 3.9. Let the metallic structure $\mathcal{J}$ be integrable on $\mathcal{M}$. Then the metallic structure $\mathcal{J}^{II}$ is integrable on $T_2(\mathcal{M})$ if and only if

$$N_{\mathcal{J}^{II}}(X^{II}, Y^{II}) = 0.$$

Proof. From the equation (19), we have

$$N_{\mathcal{J}^{II}}(X^{II},Y^{II}) = [\mathcal{J}^{II}X^{II},\mathcal{J}^{II}Y^{II}] - \mathcal{J}^{II}[\mathcal{J}^{II}X^{II},Y^{II}]$$
$$-\mathcal{J}^{II}[X^{II},\mathcal{J}^{II}Y^{II}] + (\mathcal{J}^{II})^2[X^{II},Y^{II}].$$

In view of equations (14), we have

$$N_{\mathcal{J}^{II}}(X^{II},Y^{II}) = \Big(N_{\mathcal{J}}(X,Y)\Big)^{II} = 0$$

since the golden structure $\mathcal{J}$ is integrable in $\mathcal{M}$. □

Recall (Özkan and Yılmaz, 2018) that if the metallic structure $\mathcal{J}$ is integrable then both the distributions K and L are integrable. Therefore, we give following proposition.

Proposition 3.10. If the second lift $\mathcal{J}^{II}$ of $\mathcal{J}$ is integrable on $T_2(\mathcal{M})$ then both of the distributions K^{II} and L^{II} are integrable on $T_2(\mathcal{M})$.

Let ∇ be a linear connection on $\mathcal{M}$. To the pair $(\mathcal{J},\nabla)$ we associate two other linear connections (Bejancu and Farran, 2006; Ianuş, 1971; Özkan and Yılmaz, 2018):

(i) The Schouten connection is given by

$$\tilde{\nabla}_X Y = k(\nabla_X kY) + l(\nabla_X lY).$$

(ii) The Vrănceanu connection is given by

$$\check{\nabla}_X Y = k(\nabla_{kX} kY) + l(\nabla_{lX} lY) + k[lX,kY] + l[kX,lY].$$

Let ∇ be a linear connection on $\mathcal{M}$. Then there exists a unique linear connection ∇^{II} in $T_2(\mathcal{M})$ which satisfies

$$\nabla^{II}_{X^{II}} Y^{II} = (\nabla_X Y)^{II}$$

for any $X,Y \in \chi(\mathcal{M})$ (Yano and Ishihara, 1973). Thus, to the pair $(\mathcal{J}^{II},\nabla^{II})$ we have two other linear connections on $T_2(\mathcal{M})$:

(i') The Schouten connection is given by

$$\tilde{\nabla}^{II}_{X^{II}} Y^{II} = k^{II}\big(\nabla^{II}_{X^{II}} k^{II}Y^{II}\big) + l^{II}\big(\nabla^{II}_{X^{II}} l^{II}Y^{II}\big). \tag{26}$$

(ii') The Vrănceanu connection is given by

$$\check{\nabla}^{II}_{X^{II}} Y^{II} = k^{II}\big(\nabla^{II}_{k^{II}X^{II}} k^{II}Y^{II}\big) + l^{II}\big(\nabla^{II}_{l^{II}X^{II}} l^{II}Y^{II}\big)$$
$$+k^{II}[l^{II}X^{II},k^{II}Y^{II}] + l^{II}[k^{II}X^{II},l^{II}Y^{II}]. \tag{27}$$

From (Demetrepoulou-Psomopoulou, 1988; Özkan and Yılmaz, 2018), we give the following two propositions.

Proposition 3.11. The projectors k^{II}, l^{II} are parallels with respect to Schouten and Vrănceanu connections for every linear connection ∇^{II} on $T_2(\mathcal{M})$ and $\mathcal{J}^{II}$ is parallel with respect to Schouten and Vrănceanu connections.

Proof. From (16), for $X, Y \in \chi(\mathcal{M})$, we have

$$\begin{aligned}
\left(\tilde{\nabla}^{II}_{X^{II}} k^{II}\right) Y^{II} &= \tilde{\nabla}^{II}_{X^{II}} k^{II} Y^{II} - k^{II}\left(\tilde{\nabla}^{II}_{X^{II}} Y^{II}\right) \\
&= k^{II}\left(\nabla^{II}_{X^{II}} r^{II} Y^{II}\right) - k^{II}\left(\nabla^{II}_{X^{II}} k^{II} Y^{II}\right) \\
&= 0, \\
\left(\check{\nabla}^{II}_{X^{II}} k^{II}\right) Y^{II} &= \check{\nabla}^{II}_{X^{II}} k^{II} Y^{II} - k^{II}\left(\check{\nabla}^{II}_{X^{II}} Y^{II}\right) \\
&= k^{II}\left(\nabla^{II}_{k^{II} X^{II}} k^{II} Y^{II}\right) + k^{II}[l^{II} X^{II}, k^{II} Y^{II}] \\
&\quad - k^{II}\left(\nabla^{II}_{k^{II} X^{II}} k^{II} Y^{II}\right) - k^{II}[l^{II} X^{II}, k^{II} Y^{II}] \\
&= 0
\end{aligned}$$

Similar relations hold for l^{II}.

From (15) and (17) it results that $\mathcal{J}^{II}$ is parallel with respect to Schouten and Vrănceanu connections. □

From (Demetrepoulou-Psomopoulou, 1988), we can give the following definitions.

Definition 3.12. If $\nabla^{II}_{X^{II}} Y^{II} \in \mathcal{D}^{II}$ where $X^{II} \in \chi(T_2(\mathcal{M}))$ and $Y^{II} \in \mathcal{D}^{II}$, the distribution $\mathcal{D}^{II}$ is called parallel with respect to linear connection ∇^{II} on $T_2(\mathcal{M})$.

Definition 3.13. Let ∇^{II} be a linear connection on $T_2(\mathcal{M})$. If $(\Delta \mathcal{J}^{II})(X^{II}, Y^{II}) \in K^{II}$ where

$$\begin{aligned}
&(\Delta \mathcal{J}^{II})(X^{II}, Y^{II}) = \mathcal{J}^{II} \nabla^{II}_{X^{II}} Y^{II} - \mathcal{J}^{II} \nabla^{II}_{Y^{II}} X^{II} \\
&- \nabla^{II}_{\mathcal{J}^{II} X^{II}} Y^{II} + \nabla^{II}_{X^{II}} (\mathcal{J}^{II} Y^{II}) \qquad (28)
\end{aligned}$$

for $X^{II} \in K^{II}$, $Y^{II} \in \chi(T_2(\mathcal{M}))$, the distribution K^{II} is called ∇^{II}-half parallel.

Definition 3.14. Let ∇^{II} be a linear connection on $T_2(\mathcal{M})$. If $(\Delta \mathcal{J}^{II})(X^{II}, Y^{II}) \in L^{II}$ where $X^{II} \in K^{II}, Y^{II} \in \chi(T_2(\mathcal{M}))$, the distribution K^{II} is called ∇^{II}-anti half parallel.

Proposition 3.15. The distributions K^{II}, L^{II} are parallel with respect to Schouten and Vrănceanu connections for the linear connection ∇^{II} on $T_2(\mathcal{M})$.

Proof. Let $X \in \chi(\mathcal{M})$ and $Y \in K$. Thus, $X^{II} \in \chi(T_2(\mathcal{M}))$ and $Y^{II} \in K^{II}$. Since $l^{II}Y^{II} = (lY)^{II} = 0$, $k^{II}Y^{II} = (kY)^{II} = Y^{II}$, we have

$$\tilde{\nabla}^{II}_{X^{II}}Y^{II} = k^{II}\left(\nabla^{II}_{X^{II}}Y^{II}\right) \in K^{II},$$

$$\check{\nabla}^{II}_{X^{II}}Y^{II} = k^{II}\left(\nabla^{II}_{k^{II}X^{II}}Y^{II}\right) + k^{II}[l^{II}X^{II}, Y^{II}] \in K^{II}.$$

Hence, K is parallel with respect to $\tilde{\nabla}$ and $\check{\nabla}$.

In the same manner, we can see that L^{II} satisfies the similar relations. □

Proposition X. The distributions K^{II} and L^{II} are parallel with respect to ∇^{II} linear connection if and only if ∇^{II} and $\tilde{\nabla}^{II}$ are equal.

Proof. If K^{II}, L^{II} are $\nabla^{\mathrm{II}}-$parallel then $\nabla^{\mathrm{II}}_X(k^{II}Y^{II}) \in K^{II}$ and $\nabla^{\mathrm{II}}_X(l^{II}Y^{II}) \in L^{II}$ for $X^{II}, Y^{II} \in \chi\left(T_2(\mathcal{M})\right)$. For that reason

$$\nabla^{\mathrm{II}}_{X^{II}}(k^{II}Y^{II}) = k^{II}\nabla^{\mathrm{II}}_{X^{II}}(k^{II}Y^{II}),\ \nabla^{\mathrm{II}}_{X^{II}}(l^{II}Y^{II}) = l^{II}\nabla^{\mathrm{II}}_{X^{II}}(l^{II}Y^{II}).$$

Since $k^{II} + l^{II} = I$ and from (26),

$$\nabla^{II}_{X^{II}}Y^{II} = k^{II}\nabla^{\mathrm{II}}_{X^{II}}(k^{II}Y^{II}) + l^{II}\nabla^{\mathrm{II}}_{X^{II}}(l^{II}Y^{II}) = \tilde{\nabla}^{II}_{X^{II}}Y^{II}.$$

Therefore $\nabla^{II} = \tilde{\nabla}^{II}$.

The converse can be shown easily. □

Proposition 3.16. If $[k^{II}X^{II}, l^{II}Y^{II}] \in K^{II}$ where $X^{II} \in K^{II}, Y^{II} \in \chi(T_2(\mathcal{M}))$, the distribution K^{II} is half parallel with respect to the Vrănceanu connection.

Proof. In the view of the equation (28) for $\check{\nabla}$, we have

$$l^{II}(\Delta\mathcal{J}^{II})(X^{II}, Y^{II}) = l^{II}\mathcal{J}^{II}\check{\nabla}^{II}_{X^{II}}Y^{II} - l^{II}\mathcal{J}^{II}\check{\nabla}^{II}_{Y^{II}}X^{II}$$
$$-l^{II}\check{\nabla}^{II}_{\mathcal{J}^{II}X^{II}}Y^{II} + l^{II}\check{\nabla}^{II}_{X^{II}}(\mathcal{J}^{II}Y^{II})$$

for $X^{II} \in K^{II}, Y^{II} \in \chi(T_2(\mathcal{M}))$.

Using (17) and (27), we obtain

$$l^{II}(\Delta\mathcal{J}^{II})(X^{II}, Y^{II}) = \left(a - 2\rho_{a,b}\right)l^{II}[k^{II}X^{II}, l^{II}Y^{II}]$$

which proves the proposition. □

Similarly, we have the following proposition for distribution L^{II}:

Proposition 3.17. If $[l^{II}X^{II}, k^{II}Y^{II}] \in L^{II}$ where $X^{II} \in L^{II}, Y^{II} \in \chi(T_2(\mathcal{M}))$, the distribution L^{II} is half parallel with respect to the Vrănceanu connection.

Proposition 3.18. The distributions K^{II} and L^{II} are anti half parallel with respect to Vrănceanu connection.

Proof. Taking account of the equation (28) for $\breve{\nabla}$, we obtain

$$k^{II}(\Delta\mathcal{J}^{II})(X^{II},Y^{II}) = k^{II}\mathcal{J}^{II}\breve{\nabla}^{II}_{X^{II}}Y^{II} - k^{II}\mathcal{J}^{II}\breve{\nabla}^{II}_{Y^{II}}X^{II}$$
$$-k^{II}\breve{\nabla}^{II}_{\mathcal{J}^{II}X^{II}}Y^{II} + k^{II}\breve{\nabla}^{II}_{X^{II}}(\mathcal{J}^{II}Y^{II})$$

for $X^{II} \in K^{II}, Y^{II} \in \chi(T_2(\mathcal{M}))$.

As a result, by (17) and (27), we obtain

$$k^{II}(\Delta\mathcal{J}^{II})(X^{II},Y^{II}) = \left(2\rho_{a,b} - a\right)k^{II}[l^{II}X^{II}, k^{II}Y^{II}].$$

Since $l^{II}X^{II} = 0$, we have $k^{II}(\Delta\mathcal{J}^{II})(X^{II},Y^{II}) = 0$. Hence $(\Delta\mathcal{J}^{II})(X^{II},Y^{II}) \in L^{II}$, and K^{II} is anti half parallel with respect to Vrănceanu connection.

Similarly, we can show that L^{II} is anti half parallel with respect to Vrănceanu connection. □

4. Metallic semi-Riemannian metrics in tangent bundle of order two

In this section, we investigate a metallic semi-Riemannian manifold with respect to the semi-Riemannian metric, and we give some properties of the metallic semi-Riemannian manifold.

Definition 4.1. A semi-Riemannian almost product structure is a pair (g,P) with g a semi-Riemannian metric on $\mathcal{M}$ and an almost product structure P is a g −symmetric endomorphism

$g(PX,Y) = g(X,PY)$

for $\forall X,Y \in \Im_0^1(\mathcal{M})$ (Gray, 1967; Yano and Kon, 1984).

Proposition 4.2. Let g be a semi-Riemannian metric on $\mathcal{M}$. Then g^{II} is a semi-Riemannian metric in $T_2(\mathcal{M})$ (Yano and Ishihara, 1973).

Let g a semi-Riemannian metric and P an almost product structure on $\mathcal{M}$, then the pair (g^{II},P^{II}) is a semi-Riemannian almost product structure on $T_2(\mathcal{M})$ if and only if so is (g,P). Thus, we have

$g^{II}(P^{II}X^{II},Y^{II}) = g^{II}(X^{II},P^{II}Y^{II})$.

From equations (2) and (10), we obtain following proposition.

Proposition 4.3. The almost product structure P is a g −symmetric endomorphism if and only if golden structure $\mathcal{J}^{II}$ is a g^{II} −symmetric endomorphism.

Definition 4.4. A metallic semi-Riemannian structure on $\mathcal{M}$ is a pair $(g, \mathcal{J})$ with

$$g(\mathcal{J}X, Y) = g(X, \mathcal{J}Y).$$

The triple $(\mathcal{M}, g, \mathcal{J})$ is a metallic semi-Riemannian manifold (Hreţcanu and Crasmareanu, 2013).

Proposition 4.5. If $\mathcal{J}$ is a metallic semi-Riemannian structure on $\mathcal{M}$, then the second lift $\mathcal{J}^{II}$ of $\mathcal{J}$ is a metallic semi-Riemannian structure on $T_2(\mathcal{M})$.

Corollary 4.6. Let $(\mathcal{M}, g, \mathcal{J})$ be a metallic semi-Riemannian manifold, then on a metallic semi-Riemannian manifold $(T_2(\mathcal{M}), g^{II}, \mathcal{J}^{II})$:

(i) The projectors k^{II}, l^{II} are g^{II} −symmetric endomorphism if and only if k, l are g −symmetric.

(ii) The distribution K^{II}, L^{II} are g^{II} −orthogonal if and only if K, L are g −orthogonal.

(iii) The metallic structure $\mathcal{J}^{II}$ is $N_{\mathcal{J}^{II}}$ −symmetric if and only if the metallic structure $\mathcal{J}$ is $N_{\mathcal{J}}$ −symmetric.

From (Özkan and Yılmaz, 2018), we have following proposition.

Proposition 4.7. A semi-Riemannian almost product structure is a locally product structure if P^{II} is parallel with respect to the Levi-Civita connection $\bar{\nabla}^{II}$ of g^{II}, i.e. $\bar{\nabla}^{II}P^{II} = 0$ and if ∇^{II} is a symmetric linear connection then the Nijenhuis tensor of P^{II} verifies

$$N_{P^{II}}(X^{II}, Y^{II}) = \left(\nabla^{II}_{P^{II}X^{II}}P^{II}\right)Y^{II} - \left(\nabla^{II}_{P^{II}Y^{II}}P^{II}\right)X^{II} - P^{II}\left(\nabla^{II}_{X^{II}}P^{II}\right)Y^{II} + P^{II}\left(\nabla^{II}_{Y^{II}}P^{II}\right)X^{II}.$$

Proposition 4.8. On a locally product metallic semi-Riemannian manifold, the metallic structure $\mathcal{J}^{II}$ is integrable.

By this result and from (Özkan and Yılmaz, 2018), we have following theorem.

Theorem 4.9. The set of linear connections ∇^{II} for which $\nabla^{II}\mathcal{J}^{II} = 0$ is

$$\nabla^{II}_{X^{II}}Y^{II} = \frac{1}{\left(2\rho_{a,b}-a\right)^2}[(a^2+b)\bar{\nabla}^{II}_{X^{II}}Y^{II} + 2\mathcal{J}^{II}\left(\bar{\nabla}^{II}_{X^{II}}\mathcal{J}^{II}Y^{II}\right) - a\mathcal{J}^{II}\left(\bar{\nabla}^{II}_{X^{II}}Y^{II}\right) - a\bar{\nabla}^{II}_{X^{II}}\mathcal{J}^{II}Y^{II}] + O_{P^{II}}Q^{II}(X^{II}, Y^{II})$$

where $\bar{\nabla}^{II}$ is second lift of a linear connection $\bar{\nabla}$ and Q^{II} is second lift of an $(1,2)$ −tensor field Q for which $O_P Q$ is an associated Obata operator

$O_P Q(X,Y) = \frac{1}{2}[Q(X,Y) + PQ(X,PY)]$

for the corresponding almost product structure (3).

References

Akyol, M.A., *Remarks on metallic maps between metallic Riemannian manifolds and constancy of certain maps*, Honam Mathematical J., 41(2) (2019), 343-356.

Beldjilali, G., *s-Golden manifolds*, Mediterr. J. Math., 16:56, (2019).

Beldjilali, G., *A new class of golden Riemannian manifold*, Int. Electron. J. Geom., 13(1) (2020), 1–8. [

Bejancu, A. and Farran, H.R., Foliations and Geometric Structures, *Mathematics and Its Applications*, *Vol. 580*, Springer, 2006.

Crasmareanu, M. and Hreţcanu, C.E., *Golden differential geometry*, Chaos, Solitons & Fractals, 38(5) (2008), 1229–1238.

Das, L.S., *Prolongations of F-structure to the tangent bundle of order* 2, Internat. J. Math. Sci., 16(1) (1993), 201-204.

Demetrepoulou-Psomopoulou, D., *Linear connection on manifolds admitting an $f(2v+3,-1)$-structure or an $f(2v+3,1)$-structure*, Tensor (N.S.), 47(3) (1988), 235-239.

Erdoğan, F.E., *On some types of lightlike submanifolds of golden semi-Riemannian manifolds*, Filomat, 33(10) (2019), 3231–3242.

Erdoğan, F.E., Perktaş, S.Y., Acet, B.E. and Blaga, A.M., *Screen transversal lightlike submanifolds of metallic semi-Riemannian manifolds*, Journal of Geometry and Physics, 142 (2019), 111-120.

Gezer, A., Cengiz, N. and Salimov, A., *On integrability of golden Riemannian structures*, Turk. J. Math., 37 (2013), 693-703.

Gezer, A. and Karaman, Ç., *On metallic Riemannian structures*, Turk. J. Math., 39 (2015), 954-962.

Gezer, A. and Karaman C., *Golden-Hessian structures*, Proc. Natl. Acad. Sci., India, Sect. A Phys. Sci., 86(1) (2016), 41–46.

Gray, A., *Pseudo-Riemannian almost product manifolds and submersions*, J. Math. Mech., 16(7) (1967), 715-737.

Hreţcanu, C.E., *Submanifolds in Riemannian manifold with golden structure*, Workshop on Finsler Geometry and Its Applications, Hungary, (2007).

Hreţcanu, C.E. and Crasmareanu, M., *Metallic structures on Riemannian manifolds*, Revista Union Math. Argentina, 24(2) (2013), 15-27.

Ianuş, S., *Sur Les structures presque produit des varietes a connection lineaire*, C.R.A.S. Paris, 272 (1971), 734-735.

Keçilioğlu, O., Prolongations of Hypersurfaces to Tangent Bundles of Order Two, *Ph. D. Thesis*, Gazi University Institute of Science and Technology, Ankara, 2010.

Mathai, S., *Prolongations of f −structure to tangent bundle of order* 2, Indian J. Pure Appl. Math., 6(10) (1975), 1180-1184.

Özkan, M. and Peltek, B., *Silver differential geometry*, II. International Eurasian Conference on Mathematical Sciences and Applications, Sarajevo-Bosnia and Herzegovina, 273, (2013).

Özkan, M., *Prolongations of golden structures to tangent bundles*, Diff. Geom. Dyn. Syst., 16 (2014), 227-238.

Özkan M., Çıtlak A.A. and Taylan E., *Prolongations of golden structure to tangent bundle of order 2*, GU J Sci, 28(2) (2015), 253.

Özkan, M. and Yılmaz, F., *Bronze structure*, 14th Mathematics Symposium, Niğde, (2015).

Özkan, M. and Peltek, B., *A New structure on manifolds: Silver structure*, Int. Electron. J. Geom., 9(2) (2016), 59-69.

Özkan, M. and Uz, O.E., *Complete lifts of metallic structures to tangent bundles*, 14th International Geometry Symposium, Denizli, (2016).

Özkan M., Taylan E. and Çıtlak A.A., *On lifts of silver structure*, Journal of Science and Arts, 2(39) (2017), 223-234.

Özkan, M. and Yılmaz, F., *Metallic structures on differentiable manifolds*, Journal of Science and Arts, 3(44) (2018), 645-660.

Savas, M., Özkan, M. and Iscan, M., *On 4-dimensional golden-Walker structures*, Journal of Science and Arts, 2(35) (2017), 89–100.

Spinadel, V.W., *On characterization of the onset to chaos*, Chaos, Solitons & Fractals, 8(10) (1997), 1631-1643.

Spinadel, V.W., *The family of metallic means*, Vis Math, 1., (1999). http://members.tripod.com/vismath/

Spinadel, V.W., *The metallic means family and renormalization group techniques*, Proc. Steklov Inst. Math. Control in Dynamic Systems, Suppl. 1 (2000), 194-209.

Yano, K. and Ishihara, S., *Differential geometry of tangent bundle of order 2*, Kodai Math. Sem. Rep., 20 (1968), 318-354.

Yano, K. and Ishihara, S., Tangent and Cotangent Bundle, *Marcel Dekker Inc.*, New York, 1973.

Yano, K. and Kon, M., Structures on Manifolds, *Series in Pure Mathematics, Vol. 3*, World Scientific, Singapore, 1984.

Yılmaz, F., Metallic Differential Geometry, *M. Sc. Thesis*, Gazi University Graduate School of Natural and Applied Sciences, Ankara, 2016.

CHAPTER IV

THERMAL NEUTRON FISSION OF URANIUM-233 BY MONTE-CARLO METHOD

Assist. Prof. Dr. Sevil AKÇAĞLAR
Dokuz Eylül University, İzmir, Turkey, sevil.akcaglar@deu.edu.tr
Orcid No : 0000-0002-5386-1862

1. Introduction

Nowadays the energy requirement was obtained by fossil fuels (80 %), hydraulic (10 %) and by nuclear (10 %) energies (Vorobyev et al., 2009; Wilsona et al., 2015). The environmental pollution originating from the coal and insufficient petroleum and natural gas reserves cause to utilization of nuclear energy in last decades (Shcherbakov et al., 2009; Wilsona et al., 2015). Although the capital cost of nuclear energy is high, lower fuel prices cause to economic utilization of nuclear sources. Nowadays, nuclear energy provides 10 % of the electric energy of the World (Vogta et al., 2013). The power reactors consist of natural uranium and uranium-235 and of reactors enriched with uranium fuel. In the World in the 31 country are 432 active nuclear central with a total power of 340347 MW (Vogta et al., 2013; Bergea et al., 2015). The fissile elements can be used as nuclear fuel is U-235, U-233 and U-239. The reason of expanded utilization of U-235 in the recent years is the naturel presence of U-235 in the uranium element (Sardeta et al., 2015; Ruskova et al., 2015). Nuclear fission process can be defined by the pumping of the heavily uranium elements by neutrons (Beiser, 1973; Madland, 2006; Kawano et al., 2013). In the thermal fission of U-233, in order to determine the ratio of deformation energies it was used two models namely adiabatic and statistic (Naika et al., 2013; Wilson et al., 2015), Fissile elements which can be used as nuclear energy sources are U-235, Pu-239 and U-233 (Vogta et al., 2013; Naika et al., 2013). Although, there is a lot of studies to find energy concerning the U-235 and Pu-239 limited studies were about thermal fission of U-233 (Al-Adilia et al., 2013; Pomp et al., 2015). There is no experimental and theoretical data's during thermal fission of the nucleus of U-233 to obtain nuclear energy in the literature.

In the frame work of this study, it was aimed to obtain the maximum nuclear energy by thermal neutron fission using adiabatic model in Turkey since in the future it will be used nuclear energy since

the other energy sources (coal petroleum electricity) are very limited. The calculation was performed by using Monte-Carlo Method. The goals in this study are to obtain the disturbance of secondary mass chain by calculation of independent yields of secondary products and independent yields ratio and to determine the disturbances of charge of secondary products and the most probable charge values. With the mass numbers of prompt neutron separating by the neutrons and the variation of product mass of mass center energy were investigated by using adiabatic model. In this model the ratio of deformation energies was calculated. The variation of product mass separated by the gamma beams energies and the variation of width of secondary product in the neutron fission of U-233 were determined. Furthermore, the data obtained from the Monte-Carlo Method were correlated with the other thermal fission process values and experimental studies.

2. Theoretical background

There are studies giving the product yields altogether of several fission systems which are measured with different experimental methods and calculating the most appropriate value from these experimental data (Aritomo et al., 2015). Meek and Rider have analyzed nearly 13000 product yields which are measured from several energy levels' fissions of Thorium, Uranium and Plutonium (Meek and Rider, 1974; Al-Adilia et al., 2013; Qiao et al., 2014). They have published the experimental data values considering the conditions of the experiment, the error limits and the number of repeats and decay properties of the products. Yamamato and Sugiyama have corrected the primary product yield distributions with instantaneous-neutron numbers in order to obtain the graphics of secondary product mass yields (Beiser, 1973; Yamamoto and Sugiyama, 1977; Vorobyev et al., 2009; Shcherbakov et al., 2009; Sardeta et al., 2015). The values for the slow neutron fission of U-233 founded by Yamamato are given together with Crouch's experimental data in Figure1.

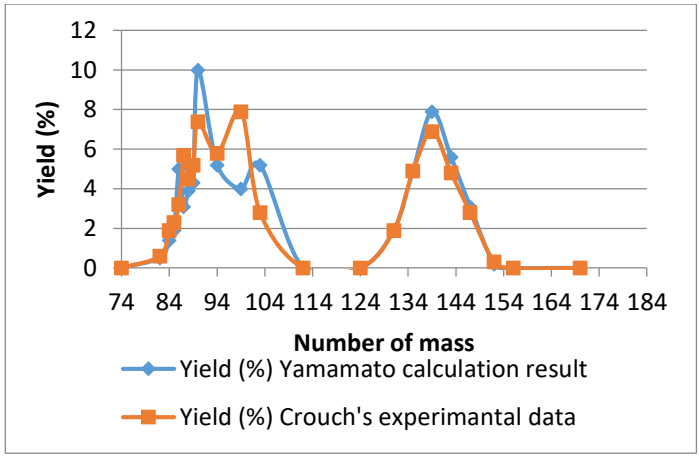

Fig. 1 The distribution of mass chain yields in the slow neutron fission of U-233.

The experimental results are described in accordance with these models by utilizing the statistical and adiabatic models for the theoretical calculations performed by Sardeta (Sardeta et al., 2015). There is a strong interaction between the collective motion of the core from the statistical model and motions of single particle. The collective motion develops quickly towards the breaking point as reported by Aritomo (Naika et al., 2013; Aritomo et al., 2015). Since the nucleons cannot follow this motion as adiabatic, a portion of the energy is transferred to the nucleons as exciting energy. Thus a balance is established between the nucleons' degrees of freedom at the breaking point and the temperatures of the products are equal at break as reported by Naika and Pomp (Naika et al., 2013; Al-Adilia et al., 2013; Wilson et al., 2015; Pomp et al., 2015). In contrast, in the division process toward the breaking point, the collective motion of the nucleus develops slowly in adiabatic model and the nucleons follow the nucleus's collective motion as adiabatic as reported by Reinhard and Goeke (Reinhard and Goeke, 1986). Under these circumstances the interaction between the nucleus's single particle motion and its collective motion is weak and the internal temperature of products at break can be considered to be zero. Until now is the fine structure that was formed with double proton nucleus. It is observed that especially possibility of double protons or double neutrons nucleus occurrence is higher as reported by Kawano and Naika (Beiser, 1973; Naika et al., 2013). Another feature observed in the yield-mass graphics is that a curve belonging to a heavy mass group does not move a lot but there are obvious shifts in the light mass groups. Another common features found in yield graphics is that

symmetric mass division possibility is low but as excitation energy goes up this possibility goes up (Wilson et al., 2015; Pomp et al., 2015). It is very important that number and energy distribution of the prompt nucleus are examined so as to explain the developments during the diversion of the nucleus in fission and due to its importance in practices (Bergea et al., 2015; Sardeta et al., 2015). First experimental study analyzing prompt neutron number product mass and change for the slow neutron fission of the U-233 nucleus was made by Fraser and Milton (Fraser and Milton, 1954; Pomp et al., 2015).

As a result of these experiments in which prompt neutrons were counted as coincidences with fission products it was founded that in a division neutron numbers of heavy and light products were different and total prompt number released product pairs determined change with mass ratio (Rubchenya et al., 2001). By many scientist's prompt neutron of each product was found with values of primary and secondary product efficiency through physical measurement. Of these, prompt neutron and yield-mass distribution of U-233 for fission by Terrell can be seen in Figure 2. In the following studies, Walsh and Boldeman analyzed the fine structure of the prompt neutron in fission, compared it with the construction in the product yield distribution and observed that for both distributions this construction was found at same mass (Terrell, 1962; Walsh and Boldeman, 1977). Adiabatic and statistical models were used for explaining results of mass related prompt neutron numbers (Chatillon et al., 2014). The most important difference between these two models is the extent of the interaction between collective character of the divided nucleus and one particle actions of the nucleons. In the adiabatic model this interaction is weak and in the statistical model the interaction is strong.

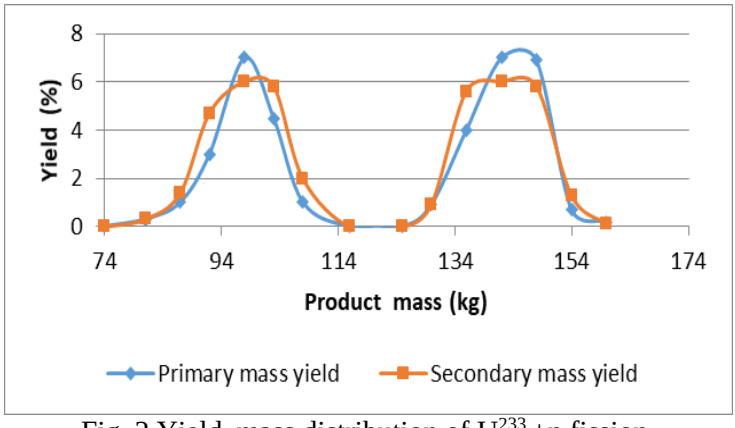

Fig. 2 Yield–mass distribution of U^{233} +n fission.

With a new approach to adiabatic model, Terrell, Kawano and Qiao suggested that deformation that divided nucleus included is depended on the features of the product (Terrell, 1962; Kawano et al., 2013; Al-Adilia et al., 2013).

2.1 Methods used in the calculations

Since neutron division from fission product is a statistical issue, for calculation of prompt neutrons' and gamma lights' average number and energy Monte-Carlo method is used. Monte Carlo method is based on Weisskopff's "nuclear evaporation" model (Nagaya et al., 2010).

2.2 Computer program used in the studies

In this study, in order to detect the product distributions during neutron fission and the prompt-neutron numbers, their energies and the gamma energies a computer mathematical program namely Fortran 4 was used.

3. Result and discussion

3.1 Primary Product Mass Chain Yield and Charge Values

For the primary fragment mass chain product and charge values of U-233, values found by Meek and Rider were used and product mass and change graphic was drawn and is shown in Figure 3 (Qiao et al., 2014; Sardeta et al., 2015; Wilson et al., 2015). The yields increased at U-233 by products 90, 99, 135 and 146, respectively.

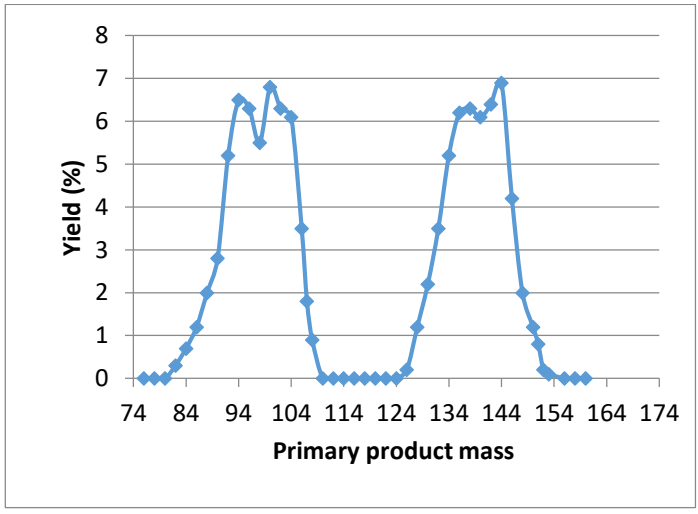

Fig. 3 U-233's primary fragment mass chain yield.

3.2 Yield of Fragment Product Mass Chain

In this study the fragment data of product mass chain and the most probable charge of fragment product mass chain (Zp) data were obtained by Meek and Rider, Wolsberg respectively (Meek and Rider,

1974; Wolfsberg et al., 1974; Naika et al., 2013; Al-Adilia et al., 2013; Qiao et al., 2014; Chatillon et al., 2014). By using Zp and primary fragment independent yield ratio (PA (Z)) data via the method namely "became distant from unchanged charge distribution" it was calculated the secondary product charge distribution. Then, it was calculated the wide parameter (c) as 0.79 by using the width parameter ($\alpha = 0.56$) obtained by Meek and Rider used in low energy fission (Shcherbakov et al., 2009; Qiao et al., 2014; Sardeta et al., 2015). Figure 4 shows the relationship between the secondary product charge and PA(Z) for mass number (A)124 during thermal fission of U-233. According to this figure it was observed that the maximum secondary product charges was obtained as 49 at a PA(Z) value of 0.65. These data are in accordance with the maximum secondary product charges and PA(Z) values found by Meek and Rider (data not shown) (Meek and Rider, 1974; Qiao et al., 2014; Aritomo et al., 2015).

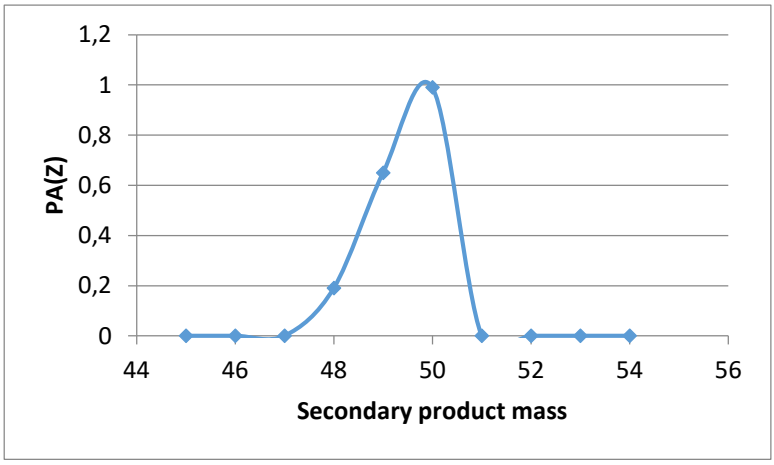

Fig. 4 Distribution of independent yield fractions for A=124 chain during U-233's prompt neutron fission.

3.3 Product yield and charge distribution of U-233 in thermal neutron fission

By multiplying the total yield of mass change (Y), and independent yield ratio PA(Z) it was calculated the ındependent yield of every isobar, the secondary product mass yield of U-233 was obtained. The relationship between mass of secondary product and percent of yield was illustrated in Figure 5 for the fission of U-233. The maximum yields of secondary product mass were 7.99 and 8.8.

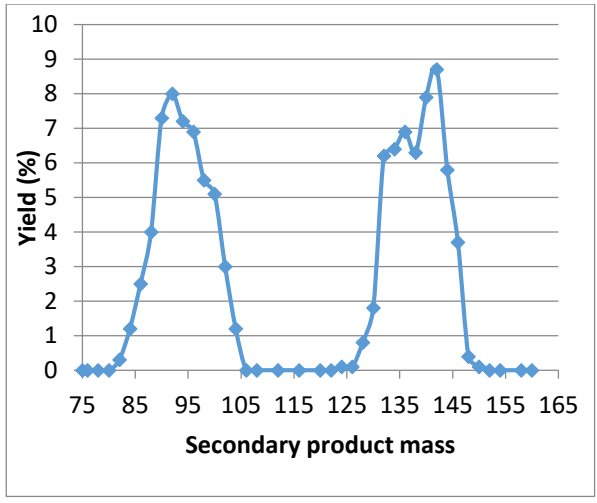

Fig. 5 Secondary product yield change with product mass during U-233's fission.

These theoretical data were correlated with the experimental studies of Crouch (Crouch et al., 1973; Kawano et al., 2013). It was found similar curves and it can be concluded that the theoretical data from our study are in accordance with the experimental results of Crouch (Figure 6) (Crouch et al., 1973; Naika et al., 2013; Pomp et al., 2015). This figure illustrates the graph between the mass number and secondary product yield (%) obtained from our theoretical data and from Crouch data (Crouch et al., 1973; Sardeta et al., 2015).

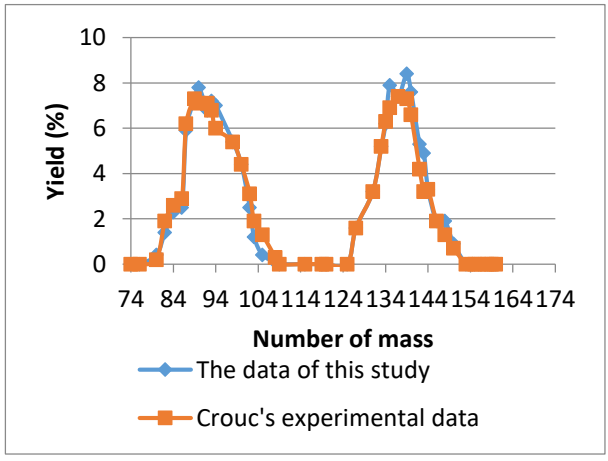

Fig. 6 Comparison of secondary product yield distribution according to product mass during U-233's fission.

In Figure 6 it was observed some thin structures in proton numbers. The maximum peaks observed in this figure can be defined as the points of mass value carrying double number of protons. As a result, it was found that the plot in Figure 6 exhibited a Gaussian distribution.

Figure 7 shows the plot between mass of secondary product and distribution of width parameter in the U-233 fission.

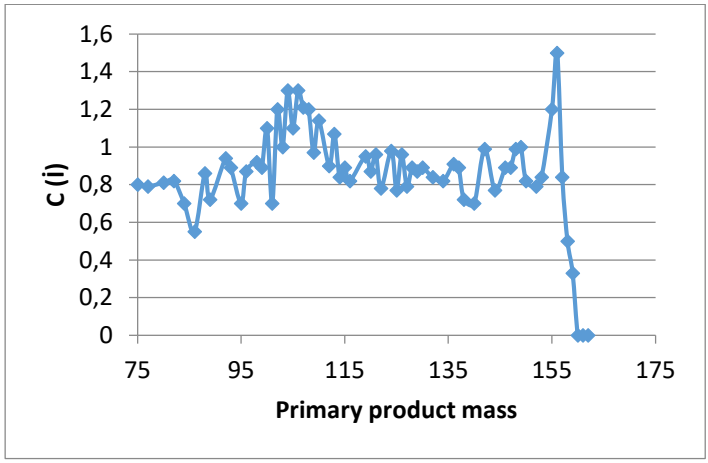

Fig. 7 Secondary product charge distribution width parameter distribution in U-233 fission.

3. 4 Disturbance of gamma and prompt neutron beams during thermal neutron fission U-233

The variation of prompt neutron numbers (VA) and variation of product mass is illustrated in Figure 8.

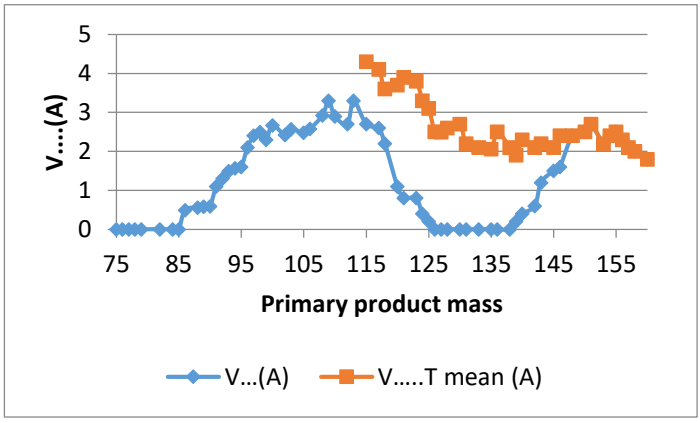

Fig. 8 Variation of the number of prompt neutrons in the fission of U-233 with product mass.

3.5 Prompt neutron numbers change with product mass in U-233 fission

In this study it was found that the theoretical prompt neutron disturbances calculated by adiabatic model are in good accordance with the experimental results found by Terrel as shown in Figure 9 (Terrell, 1962; Naika et al., 2013; Kawano et al., 2013).

In the study of Terrel the light and heavy mass groups in prompt neutron disturbance exhibited similarities with our prompt neutron disturbances (Terrell, 1962; Naika et al., 2013; Sardeta et al., 2015). The mass of products which are at the lowest neutron disturbances are placed in the region which are the masses and containing double numbers nucleon. This showed that the neutron disturbance is related with the layer structure of products.

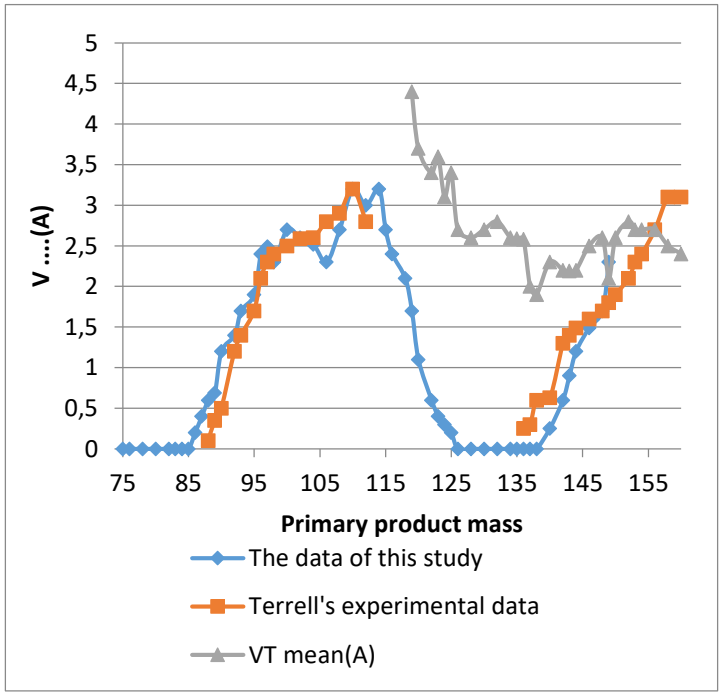

Fig. 9 Comparison of prompt neutrons change with output mass in U-233 fission.

3.6 Statistical and Evaporation Models for the neutron emission energy spectrum in the Center-Of-Mass System from fission fragments

The kinetic energies (ϵ_1) of neutron in the mass centers for each fission were calculated by Monte-Carlo Method. The kinetic energies in the laboratory system (ϵ_1) was calculated by the accepters of the neutrons were distributed isotopically. In Figure 10 the variation of product mass versus the kinetic energy in the mass center of prompt neutron was shown. The maximum kinetic energy peaks (2000-2300 MeV) are between 94 and 116 for product masses. The secondary kinetic energy peaks in the same figure reached up to 1600 MeV for product masses varying between 149 and 160.

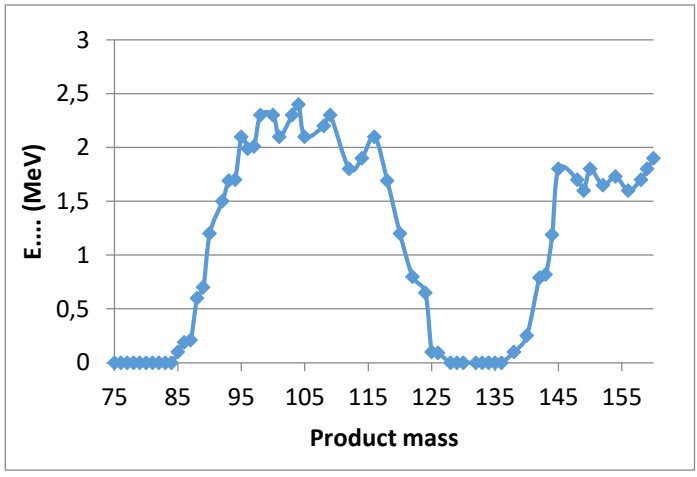

Fig. 10 Energy distribution of prompt neutrons mass center in U-233 fission.

Figure 11 shows the variation between the heavy product mass of mean total gamma beam energy separated from the fission products and the product mass of mean gamma energy during the fission of U-233 with thermal neutron. In the study Wals and Boldeman declared that double energy is very important and the numbers of prompt neutron are very related with the product charge (Walsh and Boldeman, 1977; Naika et al., 2013; Pomp et al., 2015). As illustrated in Figure 11 similar to the study of Wals and Boldeman and and Madland increases in gamma energy for products with double proton was observed (Walsh and Boldeman, 1977; Madland, 2006; Aritomo et al., 2015). As a result, according to the data obtaining of this study,

the double energy is very important in energy distribution during U-233 fission with prompt neutron.

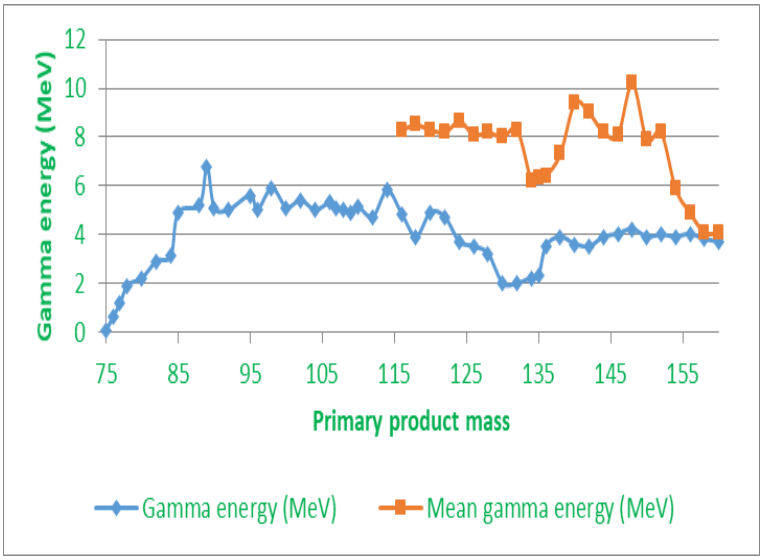

Fig. 11 γ- rays energies, released in U-233 fission, change with product mass.

4. Conclusion

The results of this study showed that general aspects for prompt neutron fission show parallelism with aspects of the studies made with Monte-Carlo calculation method. This shows that adiabatic distribution among fragments of excited energy during slow neutron fission division is also valid for U-233 fission. However, in the following studies calculations with statistical model will be made and will be analyzed comparatively.

References

Al-Adilia, A., Hambscha F.J., Pompb, S., Oberstedta, S. Corrections of prompt-neutron emission in fission-fragment experiments.; Physics Procedia 47, (2013),131–136.

Aritomo, Y., Chiba, S., Nishio, K., Independent fission yields studied based on Langevin equation. Progress in Nuclear Energy 85, (2015), 568-572.

Beiser, A., Concept of Modern Physics., Mc Graw Hill Book Company New York, (1973), USA.

Bergea, L., Litaizea, O., Serota, O., De Saint Jeana, C., Archiera, P., Peneliaua, Y., Study on Prompt Fission Neutron Spectra and

associated covariances for 235U(nth,f) and 239Pu(nth,f), Physics Procedia 64, (2015), 55 – 61.

Chatillon, A., Bélier, G., Granier, T., Laurent, B., Morillon, B., Taieb, J., by et al., Measurement of prompt neutron spectra from the 239Pu(n,f) fission reaction for incident neutron energies from 1 to 200 MeV, Phys. Rev. C 89, (2014), 014611.

Crouch, E.A.C., Paper IAEA/SM-170/94. Symposium on Applications of Nuclear Data, (1973), Paris.

Fraser, J.S. and Milton, J.C.D., Physics Review, (1954), 93-818.

Kawano, T., Talou, P., Stetcu, I., Chadwick, M.B., Statistical and evaporation models for the neutron emission energy spectrum in the center-of-mass system from fission fragments, Nuclear Physics A 913, (2013), 51–70.

Madland, D.G., Total prompt energy release in the neutron-induced fission of 235U, 238U, and 239Pu, Nuclear Physics A 772, (2006), 113–137.

Meek, M.E. and Rider, B.F., Compilation of Fission Product Yields Vallectios, Nuclear Center, NEDO- (1974), 12154-1.

Nagaya, Y., Chiba, G., Mori, T., Irwanto, D., Nakajima, K., Comparison of Monte Carlo calculation methods for effective delayed neutron fraction, Annals of Nuclear Energy, 37, 10, (2010), 1308-315.

Naika, H., Mulikb, V.K., Prajapatic, P.M., Shivasankard, B.S., Suryanarayana, S.V., Jagadeesanf, K.C., Mass distribution in the quasi-mono-energeti cneutron-induced fission of 238U, Nuclear Physics A 913, (2013), 185–205.

Pomp, S., Al-Adili, A., Alhassan, E., Gustavsson, C., Helgesson, P., Hellesen, C., by et al., Experiments and Theoretical Data for Studying the Impact of Fission Yield Uncertainties on the Nuclear Fuel Cycle with TALYS/GEF and the Total Monte Carlo Method, Nuclear Data Sheets 123, (2015), 220–224.

Qiao, Y., Zhang, M., Yang, Y., Liu, S., Wu, J., Wang, B., Determination of 235-U isotopic abundance by fission-yield difference method, Nuclear Instruments and Methods in Physics Research A 739, (2014), 44 – 47.

Reinhard, P.G., Goeke, K., Dissipative adiabatic mean field theory for large amplitude collective motion. (1986).

Rubchenya, V.A., Trzaska, W.H., Vakhtin, D.N., Äystö, J., Dendooven, P., Hankonen, S., by et al., Neutron and fragment yields in proton-induced fission of ^{238}U at intermediate energies, Nuclear Instruments and Methods in Physics, 463, 3, (2001), 653-662.

Ruskova, I., Kopatchb, Y.N., Panteleevb, Ts., Skoy, V.R., Shvetsovb, V.N., Dermendjieva, E, by et al., Prompt Gamma Emission in

Resonance Neutron Induced Fission of 239-Pu, Physics Procedia 31, (2012), 35–42.
Shcherbakov, O.A., Pleva, Y.S., Gagarski, A.M., Val'ski, G.V., Petrov, G.A., Petrova I, by et al., Measurements of angular and energy distributions of prompt neutrons from thermal neutron- Induced fission, (2009).
Sardeta, A., Graniera, T., Laurenta, B., Oberstedta, A., Experimental studies of prompt fission neutron energy spectra, Physics Procedia 47, (2013), 144–1.
Terrell, J., Neutron Yields from Individual Fission Fragments, Los Alamo Scientific laboratory university of California, Los Alamos, New Mexico, Physics Review (1962), 127-189.
Vogta, R., Randrup, J., Event-by-event modeling of prompt neutrons and photons from neutron - induced and spontaneous fission with FREYA, Physics Procedia 47, (2013), 82–87.
Vorobyev, A.S., Shcherbakov, O.A., Pleva, Y.S., Gagarski, A.M., Val'ski, G.V., Petrov, G.A., by et al., Measurements of angular and energy distributions of prompt neutrons from thermal neutron-induced fission, Nuclear Physics Institute, (2009), 188-350.
Walsh, R.L. and Boldeman, J.W., Nuclear Physics, A., (1977), 276-189.
Wilson, J.N., Leboisa, M., Halipréa, P., Oberstedtb, S., Oberstedtc, A., Scientific Workshop on Nuclear Fission dynamics and the Emission of Prompt Neutrons and Gamma Rays, Theory-3 Prompt emission in fission induced with fast neutrons, Phys.Procedia 64, (2015), 107-113.
Wolfsberg, K., LA-5553, (1974), UC-34.
Yamamoto, T. and Sugiyama, K., Report NETU-20, April (1977), Tokohu University Sendai, Japan.

Footnote: The article on "Thermal neutron fission of uranium-233 by Monte-Carlo Method", which will be published as a book chapter, has been developed and studied part of the PhD thesis.